North Atlantic Tropical Cyclone Outer Size and Structure Remain Unchanged by the Late Twenty-First Century

BENJAMIN A. SCHENKEL,[a,b] DANIEL CHAVAS,[c] NING LIN,[d] THOMAS KNUTSON,[e] GABRIEL VECCHI,[f,g] AND ALAN BRAMMER[h]

[a] *Cooperative Institute for Severe and High-Impact Weather Research and Operations, University of Oklahoma, Norman, Oklahoma*
[b] *NOAA National Severe Storms Laboratory, Norman, Oklahoma*
[c] *Department of Earth, Atmospheric, and Planetary Sciences, Purdue University, West Lafayette, Indiana*
[d] *Department of Civil and Environmental Engineering, Princeton University, Princeton, New Jersey*
[e] *NOAA Geophysical Fluid Dynamics Laboratory, Princeton, New Jersey*
[f] *Department of Geosciences, Princeton Environmental Institute, Princeton, New Jersey*
[g] *Cooperative Institute for Modeling the Earth System, Princeton University, Princeton, New Jersey*
[h] *Cooperative Institute for Research in the Atmosphere, Colorado State University, Fort Collins, Colorado*

(Manuscript received 26 January 2022, in final form 14 September 2022)

ABSTRACT: There is a lack of consensus on whether North Atlantic tropical cyclone (TC) outer size and structure (i.e., change in outer winds with increasing radius from the TC) will differ by the late twenty-first century. Hence, this work seeks to examine whether North Atlantic TC outer wind field size and structure will change by the late twenty-first century using multiple simulations under CMIP3 SRES A1B and CMIP5 RCP4.5 scenarios. Specifically, our analysis examines data from the GFDL High-Resolution Forecast-Oriented Low Ocean Resolution model (HiFLOR) and two versions of the GFDL hurricane model downscaling climate model output. Our results show that projected North Atlantic TC outer size and structure remain unchanged by the late twenty-first century within nearly all HiFLOR and GFDL hurricane model simulations. Moreover, no significant regional outer size differences exist in the North Atlantic within most HiFLOR and GFDL hurricane model simulations. No changes between the control and late-twenty-first-century simulations exist over the storm life cycle in nearly all simulations. For the simulation that shows significant decreases in TC outer size, the changes are attributed to reductions in storm lifetime and outer size growth rates. The absence of differences in outer size among most simulations is consistent with the process that controls the theoretical upper bound of storm size (i.e., Rhines scaling), which is thermodynamically invariant. However, the lack of complete consensus among simulations for many of these conclusions suggests nontrivial uncertainty in our results.

KEYWORDS: Climate change; Anthropogenic effects/forcing; Hurricanes/typhoons; Downscaling; Climate models; Tropical cyclones

1. Introduction

While changes in North Atlantic tropical cyclone (TC) intensity and track by the late twenty-first century have been well studied (Knutson et al. 2010, 2015, 2020), few studies have examined the changes in the outer size of the TC wind field. Moreover, there remains no consensus among these studies of TC outer size and structure (i.e., change in outer winds with increasing radius from the TC; Knutson et al. 2015; Yamada et al. 2017). TC outer size is defined at radii far from the storm center where winds are relatively weak and convection is minimal (Emanuel et al. 2004; Chavas et al. 2015). Understanding how TC outer size may change is also crucial for accurately predicting storm surge (Lin et al. 2014; Irish et al. 2008) and tornadoes (Paredes et al. 2021; McCaul 1991). TC outer size is linked to the structure of the inner-core wind field (Chavas and Emanuel 2014; Chavas et al. 2015), including the radius of maximum wind (Chavas and Knaff 2022), the minimum central pressure (Chavas et al. 2017), rapid intensity changes (Chen et al. 2011; Carrasco et al. 2014) and the forecasts of rapid intensification (Knaff et al. 2018, 2020), and the resilience of TC intensity and structure to vertical wind shear (Jones 1995; DeMaria 1996). Moreover, the broad horizontal scale of TC outer size is reasonable to resolve (e.g., ~400-km radius) given the current configuration of TC-resolving global climate model and downscaling climate simulations (Knutson et al. 2015; Schenkel et al. 2018). Hence, our study investigates whether projected North Atlantic outer size and structure change by the late twenty-first century using simulations from a fine-horizontal-grid-spacing global climate model and a downscaling regional hurricane model.

To understand how outer size may change by the late twenty-first century, it is first important to discuss the characteristics and life cycle of TC outer size in the current climate. Unlike TC intensity, a variety of subjectively derived wind

Denotes content that is immediately available upon publication as open access.

Supplemental information related to this paper is available at the Journals Online website: https://doi.org/10.1175/JCLI-D-22-0066.s1.

Corresponding author: Benjamin A. Schenkel, benschenkel@gmail.com

DOI: 10.1175/JCLI-D-22-0066.1

and pressure metrics have been used to define storm outer size. Most outer size metrics are characterized by a lognormal distribution with positive skewness and large variability (Chavas and Emanuel 2010; Chavas et al. 2016). The large variability of the outer size is due to two factors: 1) large differences in TC outer size at genesis (Cocks and Gray 2002; Lee et al. 2010; Chavas and Emanuel 2010; Chavas et al. 2016; Schenkel et al. 2018) and 2) typically more rapid growth of initially larger TCs (Lee et al. 2010; Xu and Wang 2010; Schenkel et al. 2018; Martinez et al. 2020). More broadly, TC outer size is smallest at genesis and then tends to grow slowly thereafter (Cocks and Gray 2002; Chavas and Emanuel 2010). Prior work has suggested that genesis TC outer size may be associated with the horizontal scale of its precursor disturbance (Rotunno and Emanuel 1987; Cocks and Gray 2002; Lee et al. 2010). However, both the magnitude and duration of outer size growth varies among basins with North Atlantic TCs characterized by longer periods of more gradual growth compared to western North Pacific storms (Schenkel et al. 2018). In both basins, TC outer size varies more slowly than intensity as shown by weak correlations between the two ($R \sim 0.3$; Merrill 1984; Chavas et al. 2016). In the North Atlantic and western North Pacific basins, the largest TCs typically are the longest-lived and traverse the greatest distances often associated with recurvature into the midlatitudes (Merrill 1984; Schenkel et al. 2018). Last, the end of the TC life cycle is characterized either by contraction of TC outer size in association with cyclolysis over the ocean or landfall (Chen and Chavas 2020; Hlywiak and Nolan 2021) or by no systematic change in association with extratropical transition followed by potential growth in outer size thereafter (Hart et al. 2006; Schenkel et al. 2018). However, the evolution of TC outer size and structure during and after extratropical transition may be sensitive to the definition used (Hart 2003; Kofron et al. 2010).

While the above work suggests that TCs tend to grow with time during their life cycle, prior work has not understood until recently which factors control outer size. Idealized simulations on the f plane have shown that a TC tends to expand rapidly with time toward an equilibrium outer size (Martinez et al. 2020; Chavas and Vigh 2014), which scales approximately with the ratio of the potential intensity to the Coriolis parameter, V_p/f (Wang et al. 2022). On the rotating sphere, Chavas and Reed (2019) used aquaplanet experiments to show that median storm outer size at low latitudes scales with a second length scale, called the Rhines scale. The Rhines scale is inversely proportional to the square root of the planetary vorticity gradient (β). This scale is associated with the generation of planetary Rossby waves by eddies that arose originally from geostrophic turbulence theory (Rhines 1975). Lu and Chavas (2022) demonstrated how wave effects act to shrink the outer circulation of a TC-like vortex toward its internal vortex Rhines scale, with larger TCs shrinking faster. Hence, the Rhines scale represents a process that reduces the natural expansion rate of TCs, an effect that is stronger for larger TCs. This process shifts the statistics of TC outer size toward smaller sizes, rather than representing an absolute scale for the size of an individual TC. Because the Rhines scale is much smaller than V_p/f at low latitudes (Chavas and Reed 2019), the TC outer size on Earth is expected to be strongly limited by the Rhines scale. This is consistent with the finding in observations that most TCs are much smaller than V_p/f (Chavas et al. 2016). Moreover, the Rhines scale slowly increases with latitude, which is consistent with observed outer size remaining constant or slowly increasing with latitude (Merrill 1984; Chavas et al. 2016). These results also suggest that the outer size of TC precursor disturbances (e.g., easterly wave) is also limited by this scale given its applicability to all eddies (Held and Larichev 1996; Lu and Chavas 2022). Indeed, a recently developed diagnostic framework used to understand large-scale climate controls on the number of TCs relative to the number of precursor disturbances implicitly suggests that disturbances are more likely to develop if they are smaller than the Rhines scale (Hsieh et al. 2020; Yang et al. 2021).

In addition to the current climate, the Rhines scale may also help understand the physics of projected changes in the TC outer size distribution due to anthropogenic climate change. Specifically, the Rhines scale depends principally on β, which is invariant thermodynamically; hence, outer size may be expected not to change strongly in a future warmer climate. Such a result would be consistent with the finding that outer size does not change strongly with warming in aquaplanet experiments with uniform thermal forcing (Stansfield and Reed 2021). We test this hypothesis here as a means to provide a greater physical interpretation of our results and as the first application of the Rhines scale to current and future climate projections of TC outer size.

Prior analyses of both observed and projected North Atlantic TC activity have yielded conflicting results on whether there have been or will be changes in storm outer size and structure. Both satellite and reanalysis-based North Atlantic TC outer size estimates show no changes during the satellite era (i.e., ~1979–present; Knaff et al. 2014; Schenkel et al. 2017; Mok et al. 2018; Zhang and Chan 2022). With regards to model projected changes, we are aware of only a small number of studies analyzing TC outer size in the late twenty-first century, which came to disparate conclusions using different simulation configurations. Despite the use of coupled and uncoupled simulations, the use of the former may be particularly important for late-twenty-first-century outer size projections given the association between TC outer size and relative SSTs (Lin et al. 2015; Chavas et al. 2016). Beginning with the uncoupled simulation studies, Stansfield et al. (2020) ran a set of uncoupled global climate model simulations under Coupled Model Intercomparison Project phase 5 (CMIP5) representative concentration pathway (RCP) 4.5 (i.e., carbon emissions decrease and stabilize before 2100) and 8.5 climate change scenarios [i.e., similar to the CMIP6 Shared Socioeconomic Pathways (SSP) 5 scenario, where carbon emissions continue increasing to 2100] for the late twenty-first century (Taylor et al. 2012). These simulations showed a shift in North Atlantic TC outer size distribution to larger values with increased anthropogenic warming (Stansfield et al. 2020). In contrast, Yamada et al. (2017) used a global atmospheric model coupled to a slab ocean model with nudged SSTs [i.e., the Nonhydrostatic Icosahedral Atmospheric Model (NICAM); Tomita and Satoh 2004]. SSTs in the model were nudged toward a climate

change scenario derived from a CMIP3/A1B scenario multimodel ensemble. In that scenario, carbon emissions start to decrease but do not stabilize before 2100, which is similar to the CMIP5/RCP6.0 climate change scenario. The CMIP3/A1B scenario of SST changes and CO_2 concentration changes were added to repeating annual cycles of observed CO_2 and SSTs from the current climate used in the control simulation. This experiment showed statistical increases in global TC outer size, but with substantial differences among basins including no statistical changes in the North Atlantic. Yamada et al. (2017) also concluded that the increases in TC outer size were associated with the most intense TCs (i.e., mean sea level pressure $<$ 980 hPa). Kreussler et al. (2021) examined both coupled and uncoupled fine-horizontal-grid-spacing global model simulations from the CMIP6 SSP5 (Haarsma et al. 2016), which showed no changes in integrated kinetic energy (i.e., proxy for TC outer size; Powell and Reinhold 2007).

With regard to fully coupled simulation results, a global climate model simulation of conditions similar to the year 1990 showed that TC outer size showed small yet significant increases within most basins when CO_2 concentrations were doubled (Kim et al. 2014). Knutson et al. (2015) downscaled uncoupled global climate model data (GFDL High-Resolution Atmospheric Model; HiRAM; Zhao et al. 2009) into the GFDL regional coupled hurricane model. These simulations use a CMIP5/RCP4.5 climate change scenario for the late twenty-first century added onto a repeating identical cycle of radiation and sea surface temperatures (SSTs). This study showed no significant changes in global TC outer size, although individual basins showed substantial differences. In particular, median North Atlantic TC outer size statistically increased by 11%. Finally, a set of idealized aquaplanet simulations run with a range of uniform SSTs show a broader TC outer size distribution with no significant changes in the median value with increasing SSTs (Stansfield and Reed 2021).

Given the discrepancies between these prior studies, it is useful to revisit TC outer size changes in greater depth using a newer class of models and the benefit of recent advances in our theoretical understanding of TC outer size. Hence, we employ data from a high-resolution global model and expanded sets of downscaling regional hurricane simulations to examine how North Atlantic TC outer size and structure are projected to change by the late twenty-first century (i.e., 2081–2100). This study focuses on TC outer size, which remains understudied compared to other characteristics (e.g., TC intensity; Knutson et al. 2020). We hypothesize that TC outer size remains unchanged by the late twenty-first century based on expectations from the Rhines scale, which is insensitive to temperature and moisture changes. Our manuscript considers two sets of anthropogenic climate change scenarios and models forced with and without present-day climate variability. As a simplifying assumption, our study does not consider how changes to internal climate variability (i.e., climate modes including El Niño–Southern Oscillation) by the late twenty-first century may impact TC outer size, which is reserved for a future study. We consider that future projections of changes in boundary conditions affecting TCs are relatively more confident for changes in time mean conditions than for changes in interannual variability of those conditions. This study will address the following motivating questions:

1) Is there a consensus among multiple models on whether projected TC outer size and structure change between the current and late-twenty-first-century climate in the North Atlantic?
2) Are changes in TC outer size and structure confined to certain portions of the TC life cycle?
3) Do changes in TC outer size and structure occur only in certain regions of the North Atlantic?

The results of this study are also crucial for improving risk assessments of landfalling TCs in future climates.

2. Data and methods

a. Climate model data

This study employs three sets of fine-horizontal-grid-spacing model simulations for present-day (control) and a late-twenty-first-century simulation (Knutson et al. 2015; Murakami et al. 2015; Knutson et al. 2022):

1) *GFDL High-Resolution Forecast-Oriented Low Ocean Resolution model (HiFLOR):* 70-yr ~25 km × ~25 km coupled global model simulation (Murakami et al. 2015). For the current climate (control) simulation, a repeating identical cycle of radiative forcing from 1995 is used with SSTs that are nudged on a 5-day time scale toward a varying monthly 1986–2005 climatology computed from mean UK Met Office Hadley Centre SST data (Rayner et al. 2003). Late-twenty-first-century simulations consist of 2081–2100 CMIP5/RCP4.5 (Taylor et al. 2012) multimodel mean SST and radiative forcing anomalies added to the control simulation initial and boundary conditions (Bhatia et al. 2018). TC genesis in HiFLOR is defined when a TC attains an upper-tropospheric warm core and tropical storm intensity ($V_{max} > 34$ kt; 1 kt $\approx$ 0.51 m s^{-1}) for at least 24 consecutive hours. HiFLOR TCs are subsequently tracked using a combination of upper-tropospheric temperature anomalies and mean sea level pressure (Murakami et al. 2015; Harris et al. 2016; Murakami et al. 2016).
2) *GFDL hurricane model downscaling with GFDL High-Resolution Atmospheric Model (HiRAM) data:* TCs from 20-yr simulations of 50 km × 50 km HiRAM model (Zhao et al. 2009) are downscaled by the 2012 operational version of the GFDL regional hurricane model (Knutson et al. 2015). HiRAM is an uncoupled atmospheric model forced with a repeating identical cycle of radiative forcing and SSTs computed using a monthly mean climatology from 1982 to 2005 calculated using the Met Office Hadley Centre dataset (Zhao et al. 2009). The late-twenty-first-century simulation is a downscaling from a HiRAM simulation run with the control conditions plus the difference between 2081–2100 and 2001–20 conditions from a 13-member multimodel mean using CMIP5/RCP4.5 conditions (Knutson et al. 2015). The regional hurricane model consists of the Princeton Ocean Model initialized with a temperature and salinity climatology from the U.S.

Navy Generalized Digital Environmental Model (GDEM) and a triply nested atmospheric model with a ~6 km × ~6 km inner storm-following nest (Bender et al. 2007). Both sets of GFDL hurricane model simulations are directly initialized, without vortex bogussing, from the boundary and initial conditions with spinup only for the ocean model, which is used to generate a cold wake (to the degree one is simulated by the model) for the ocean model initial conditions (Bender et al. 2007). Each TC simulation begins when the storm first reaches tropical storm intensity in HiRAM ($V_{max} \geq 34$ kt) and ends 1) due to cyclolysis, 2) because the TC moves poleward of 43°N, or 3) after 15 days of simulation time (Knutson et al. 2015). In both sets of GFDL simulations, the northern boundary of the simulations is at a latitude where most TCs have either started or completed extratropical transition, although there remains uncertainty on whether the starting latitude of transition will shift poleward by the late twenty-first century (Hart and Evans 2001; Liu et al. 2017; Michaelis and Lackmann 2019). A study of TC outer size and structure changes during extratropical transition by the late twenty-first century is reserved for future work.

3) *GFDL hurricane model downscaling with Zetac regional model data:* TCs from the 18-km × 18-km Zetac regional model (Knutson et al. 2007) are downscaled into the 2006 operational version of the GFDL regional hurricane model with a ~9 km × ~9 km inner nest (Knutson et al. 2022). Zetac is an uncoupled regional atmospheric model forced with initial and boundary conditions for both the atmosphere and SSTs from the 6-h National Centers for Environmental Prediction (NCEP)–National Center for Atmospheric Research (NCAR) reanalysis from 1980 to 2006 (Kalnay et al. 1996). The interior domain is spectrally nudged toward reanalysis data that have been filtered to retain only zonal and meridional wavenumbers 0–2 on a 12-h time scale (Knutson et al. 2007, 2022). Two sets of late-twenty-first-century anthropogenic climate change scenario simulations are conducted: 1) the CMIP5/RCP4.5 scenario (Taylor et al. 2012) and 2) the CMIP3/A1B scenario (Meehl et al. 2007). The CMIP5 simulation is a downscaling from a Zetac simulation run with the control conditions plus the difference between 2081–2100 and 2001–20 computed from a 13-member multimodel mean under a CMIP5/RCP4.5 scenario (Knutson et al. 2015). The CMIP3 simulation is a downscaling from control conditions plus the difference between 2081–2100 and 2001–20 under the CMIP3/A1B scenario from both an 18-member multimodel mean as well as 10 individual model members (Knutson et al. 2022). The conditions for the start and finish of each TC simulation are identical to the HiRAM-downscaling simulations except for a farther equatorward latitude threshold (i.e., ≤39°N). The differences in the initial and boundary conditions are likely the primary reason for any discrepancies between the GFDL hurricane model simulations, although differences in model configuration (e.g., horizontal grid spacing) may also be important (Knutson et al. 2015, 2022).

Prior work has shown that the magnitude and interbasin variability of the outer size and structure of TC wind and rainfall within these models fall within reasonable expectations from observations and reanalyses (Knutson et al. 2015; Murakami et al. 2015; Knutson et al. 2022). However, the simulated TCs have weaker winds and a broader radius of maximum wind for a given minimum sea level pressure due partially to the relatively coarse horizontal grid spacing used in this study, especially in HiFLOR (e.g., Fig. S1 in the online supplemental material; Walsh et al. 2007; Davis 2018). Despite this limitation, we have confidence in the use of these simulations since 1) TC outer size evolves largely independently of either TC intensity and the radius of maximum wind (Merrill 1984; Chavas and Lin 2016); 2) the broader horizontal scale of TC outer size, compared to TC intensity or radius of maximum winds, is resolvable by reanalyses and models used here (Schenkel et al. 2017, 2018); 3) strong similarity exists in both the magnitude and lifetime variability of TC outer size in HiFLOR and the GFDL hurricane model compared with reanalyses and likely QuikSCAT as well (Schenkel et al. 2017, 2018); and 4) the focus of this study is on differences in TC outer size and structure between the current and future climate rather than their fidelity compared to observations. The present study also includes the distribution of lifetime maximum intensity (see Fig. S2 in the online supplemental material) for comparison with the TC outer size results even though the former is not the focus of this study. These results project a shift in intensity toward stronger TCs in most simulations, especially at the extreme end of the intensity distribution. In contrast, lifetime maximum outer size remains unchanged (to be shown) consistent with previously documented differences in the dynamics of inner versus outer TC winds (Emanuel et al. 2004; Chavas et al. 2015).

Our analysis only includes 6-h TC track points ≤39°N for consistency among models. The HiFLOR and the GFDL hurricane model simulations have several differences in model configuration and components, which are listed in Tables 1 and 2, respectively. None of these models simulate a particular observed TC; rather, they provide dynamically consistent realizations of current climate statistics (Murakami et al. 2015; Knutson et al. 2015, 2022). In particular, the Zetac-downscaling simulations contain current climate variability due to the use of large-scale spectral nudging and the use of time-evolving uncoupled SSTs from the NCEP–NCAR reanalysis in the parent model (Knutson et al. 2013, 2022). In contrast, the variability within the remaining two models is associated with modeled atmospheric internal variability through the imposition of repeating identical cycles of climatological radiation and SSTs, although there are differences in how the latter is imposed (i.e., coupled in HiFLOR versus uncoupled in HiRAM; Knutson et al. 2015; Murakami et al. 2015).

b. *Reanalysis data*

To compare TC outer size from current climate simulations, we use observed TCs with outer size data obtained from the 6-h ~31 km × ~31 km ECMWF fifth-generation reanalysis

TABLE 1. Salient details for each dataset used in this study. For the number denoting the native grid spacing, T refers to the mean wave truncation number, C refers to the number of points across each model tile for a cubed sphere grid, and L refers to the number of vertical levels.

Model	Native grid spacing	Boundary conditions	Period	TC life cycle	Citation
ERA5	T639 L137	Observed SSTs and radiation from 1982 to 2006	25 years	Complete	Hersbach et al. (2020)
GFDL HiFLOR model	C384 L32	Current (control): Repeating 1995 conditions Future (CMIP5/RCP4.5): Current plus CMIP5 multimodel mean anomalies	50 years	Complete	Murakami et al. (2015)
GFDL hurricane model—Zetac	~9 km × ~9 km L42	Current (control): Downscaling of GFDL Zetac model using GFDL hurricane model; 1980–2006 time-evolving conditions Future (CMIP5/RCP4.5): Current, but with Zetac regional model run with 1980–2006 time-evolving conditions plus CMIP5 multimodel mean anomalies Future (CMIP3/A1B; similar to CMIP5/RCP6.0 forcing): Current, but with Zetac regional model run with 1980–2006 time-evolving conditions plus CMIP3 multimodel mean anomalies or anomalies of 10 individual CMIP3 models	27 years	15-day simulation	Knutson et al. (2022)
GFDL hurricane model—HiRAM	~6 km × ~6 km L42	Current (control): Downscaling of GFDL HiRAM model using 1982–2005 mean conditions Future (CMIP5/RCP4.5): Current plus CMIP5 multimodel mean anomalies	20 years	15-day simulation	Knutson et al. (2015)

(ERA5; Hersbach et al. 2020). However, TC outer size from the GFDL hurricane model is broader than the ERA5 due to the use of winds from the lowest model level in the former dataset, which is at a higher vertical level within the boundary layer than the ERA5. The justification for using these GFDL hurricane model data is discussed in the subsection to follow. Observed TC track data are obtained from the International Best Track Archive for Climate Stewardship, version 4, revision 0

TABLE 2. Description of ERA-5, HiFLOR, and GFDL hurricane model components used in this study.

Model	Dynamics	Radiation	Convection	Microphysics
ERA5	Global semi-Lagrangian spectral model (Diamantakis and Magnusson 2016)	Monte Carlo independent column approximation and Rapid Radiative Transfer Model for GCMs (Morcrette et al. 2008)	Modified Tiedtke scheme (Tiedtke 1989)	Single-moment, bulk microphysics (Forbes et al. 2011)
GFDL HiFLOR model	Global finite volume model (Lin 2004)	Full longwave and shortwave radiation with interactive clouds and aerosols (Freidenreich and Ramaswamy 1999; Schwarzkopf and Ramaswamy 1999)	Relaxed Arakawa–Schubert scheme (Moorthi and Suarez 1992)	Single-moment, bulk microphysics (Rotstayn 1997)
GFDL hurricane model	Regional primitive equation model using box method (Kurihara et al. 1998)	Full longwave and shortwave radiation with interactive clouds (Lacis and Hansen 1974; Schwarzkopf and Fels 1991)	Simplified Arakawa–Schubert scheme (Pan and Wu 1995)	Double-moment, bulk microphysics (Ferrier 2005)

(IBTrACS; Knapp et al. 2010). Our study focuses on TCs from 1982 and 2006 to approximately correspond with the period used for the initial and boundary conditions for the climate model simulations. We only examine those 6-h TC track points equatorward of 39°N for consistency with the climate model simulation data. We define TC genesis when the IBTrACS TC has reached or exceeded tropical storm intensity ($V_{max} \geq 34$ kt), similar to the climate model data. Previous research has shown that TC track and outer wind field size and structure are typically well represented in the North Atlantic within reanalyses (Schenkel and Hart 2012; Schenkel et al. 2017). In particular, there is a slight small bias in ERA5 outer size (Bian et al. 2021; Zhang and Chan 2022). Indeed, recent work has used reanalyses to study TC outer size and structure in the North Atlantic and western North Pacific (Schenkel et al. 2018; Mok et al. 2018; Bian et al. 2021). Additional information on the ERA5 is included in Table 1.

Following prior work (Schenkel et al. 2017, 2018), a two-step vortex recentering algorithm is used to locate the reanalysis TC center due to uncertainties both in the best track and reanalyses (Schenkel et al. 2012; Torn and Snyder 2012). First, the IBTrACS position is used as the first guess. Second, the reanalysis TC location is computed as the mean center of mass surrounding the IBTrACS location of six different variables including 700- and 850-hPa geopotential height, 700-, 850-, and 925-hPa relative vorticity, and mean sea level pressure (Brammer 2017; Marchok 2002).

c. TC outer size metric

This study uses the radius at which the azimuthal-mean near-surface (typically 10-m height) azimuthal wind is less than or equal to 8 m s^{-1} (r_8). This metric is chosen for consistency with prior work (Chavas et al. 2016; Schenkel et al. 2018) and since it is well represented compared to other outer size metrics in reanalyses albeit with a bias toward smaller values (Schenkel et al. 2017; Bian et al. 2021). Our analysis uses r_8 instead of commonly used operational metrics either from reanalyses or the best track for several reasons [e.g., the radius at which azimuthal-mean 10-m azimuthal wind equals 34 kt (r_{34})]. First and foremost, the horizontal grid spacing of the reanalysis and, to a lesser extent, HiFLOR may be too coarse to resolve a reasonable r_{34}, especially for small TCs (Schenkel et al. 2017; Bian et al. 2021). Second, r_8 in reanalyses compares well to QuikSCAT data because it is far enough from the TC center to be well resolved, while at a sufficiently high wind speed to avoid noise associated with ambient winds (Schenkel et al. 2017; Bian et al. 2021). Last, prior work has shown that r_8 yields qualitatively similar conclusions to r_{34} (Schenkel et al. 2018). This study follows the methodology of Chavas and Vigh (2014) in deriving r_8 for both reanalysis and climate model output: 1) near-surface wind vectors are spatially interpolated to a TC-relative polar coordinate excluding all points over land; 2) the TC wind is then isolated by subtracting the environmental wind which is assumed to empirically correspond to the TC translation vector multiplied by a factor of 0.55 and rotated cyclonically by 20° (Lin and Chavas 2012); 3) the azimuthal-mean azimuthal wind is computed and interpolated to a coordinate with a radial grid spacing of 0.5 times the model horizontal grid; and 4) r_8 is defined as first grid point outside the radius of maximum wind where the azimuthal wind is less than or equal to 8 m s^{-1} (Schenkel et al. 2017, 2018). The sample sizes of 6-h r_8 data for the reanalysis and each simulation are given, with their abbreviations, in Table 3. Our analysis only examines r_8 in which the TC center and most of its circulation is over water and maximum azimuthal-mean 10-m wind (v^*_{max}) $\geq$ 15 m s^{-1} (Chavas et al. 2016; Schenkel et al. 2018), which is defined as follows (Lin and Chavas 2012; Chavas et al. 2015):

$$v^*_{max} = 0.8(V_{max} - 0.55V_{trans}), \quad (1)$$

where V_{max} is the maximum 10-m wind speed, 0.8 is an empirically estimated scaling factor from Chavas et al. (2016) used to derive v^*_{max} from V_{max}, and V_{trans} is the translation speed of the TC. The term v^*_{max} is used both to exclude weak TCs embedded in strong environmental flow and for consistency with prior work (Chavas et al. 2016; Schenkel et al. 2018).

Both the magnitude and life cycle of TC outer size in the HiFLOR control simulation compare well with ERA5 (Schenkel et al. 2018). For the GFDL hurricane model, our study used wind data at the lowest model level to define outer size corresponding to a ~35-m height since 10-m data for the entire wind field in and around the storm are unavailable, whereas 10-m data are available from HiFLOR. This results in median azimuthal-mean azimuthal winds that are 10%–20% stronger in the GFDL hurricane model (i.e., 35-m data) than either HiFLOR or ERA-5 (i.e., 10-m data; shown later) consistent with expectations from observations (Franklin et al. 2003; Powell et al. 2003). However, this issue likely does not impact our primary objective for three reasons. First, we are focused on whether there are statistically significant differences in outer size and structure between the current and future climates rather than how their magnitude compares to observations (Knutson et al. 2015). Second, the weak wind speed regimes in the TC outer region at a 35-m height are likely not associated with large variability in 10-m reduction factors with radius. This suggests that the radial structure of the azimuthal-mean wind field and its outer size estimates will be similar between 35- and 10-m heights (Franklin et al. 2003; Powell et al. 2003). Third, prior work has used the lowest model wind from the GFDL hurricane model for comparison with 10-m wind data as an approximation (Knutson et al. 2015).

d. Exclusion of extratropical transition

This manuscript focuses on the portion of the TC life cycle before the onset of extratropical transition. The transition of the TC is associated with substantial changes in structure and energetics (Jones et al. 2003), although the outer size of the lower-tropospheric wind field typically remains unchanged in the North Atlantic (Schenkel et al. 2018). The start of extratropical transition is defined when the TC acquires sufficient lower-tropospheric frontal structure while retaining its lower-tropospheric warm core (Hart and Evans 2001; Evans et al. 2017). Using the cyclone phase space, transition start is quantified as when storm motion–relative lower-tropospheric (i.e.,

TABLE 3. Simulation name, abbreviation, and the numbers of North Atlantic TCs and 6-h times in which r_8 is defined in each simulation.

Simulation	Abbreviation	No. of TCs	No. of 6-h times
ECMWF fifth-generation reanalysis	ERA5	122	2007
HiFLOR—Current climate (control)	HiFLOR control	402	8000
HiFLOR—Late twenty-first century (CMIP5/RCP4.5 multimodel mean)	HiFLOR CMIP5/RCP4.5	491	9841
HiRAM-downscaling GFDL hurricane model—Current climate (control)	HiRAM control	191	4029
HiRAM-downscaling GFDL hurricane model—Late twenty-first century (CMIP5/RCP4.5 multimodel mean)	HiRAM CMIP5/RCP4.5	167	3527
Zetac-downscaling GFDL hurricane model—Current climate (control)	Zetac control	198	4680
Zetac-downscaling GFDL hurricane model—Late twenty-first century (CMIP5/RCP4.5 multimodel mean)	Zetac CMIP5/RCP4.5	183	3945
Zetac-downscaling GFDL hurricane model—Late twenty-first century (CMIP3/A1B 18-member multimodel mean)	Zetac CMIP3/A1B mean	171	4064
Zetac-downscaling GFDL hurricane model—Late twenty-first century (CMIP3/A1B Geophysical Fluid Dynamics Laboratory Climate Model, version 2.1)	Zetac CMIP3/A1B CM2.1	206	4305
Zetac-downscaling GFDL hurricane model—Late twenty-first century (CMIP3/A1B Max Planck Institute Earth System Model, low-resolution MRI-CGCM3 Meteorological Research Institute Coupled Atmosphere-Ocean)	Zetac CMIP3/A1B MPI	141	2889
Zetac-downscaling GFDL hurricane model—Late twenty-first century (CMIP3/A1B Hadley Centre Coupled Model, v3)	Zetac CMIP3/A1B HadCM3	92	1638
Zetac-downscaling GFDL hurricane model—Late twenty-first century (CMIP3/A1B Meteorological Research Institute Coupled Atmosphere–Ocean General Circulation Model, v3)	Zetac CMIP3/A1B MRI	184	3656
Zetac-downscaling GFDL hurricane model—Late twenty-first century (CMIP3/A1B Geophysical Fluid Dynamics Laboratory Climate Model, v2.0)	Zetac CMIP3/A1B CM2.0	241	4949
Zetac-downscaling GFDL hurricane model—Late twenty-first century (CMIP3/A1B Hadley Centre Global Environment Model, version 1)	Zetac CMIP3/A1B HadGEM1	78	1186
Zetac-downscaling GFDL hurricane model—Late twenty-first century (CMIP3/A1B Model for Interdisciplinary Research on Climate, v3.2, high resolution)	Zetac CMIP3/A1B MIROC-hi	122	2517
Zetac-downscaling GFDL hurricane model—Late twenty-first century (CMIP3/A1B Model for Interdisciplinary Research on Climate, v3.2, medium resolution)	Zetac CMIP3/A1B MIROC-med	185	4525
Zetac-downscaling GFDL hurricane model—Late twenty-first century (CMIP3/A1B Community Climate System Model, v3)	Zetac CMIP3/A1B CCSM3	163	3431
Zetac-downscaling GFDL hurricane model—Late twenty-first century (CMIP3/A1B Instituto Nazionale di Geofisica e Vulcanologia model)	Zetac CMIP3/A1B INGV	124	2461

900–600-hPa) layer thickness exceeds an empirically defined threshold of 10 m (i.e., B-parameter > 10 m) indicative of warm and/or moist air downstream, and cold and/or dry air upstream (Hart 2003; Evans and Hart 2003). The B-parameter is calculated using data from 900 to 600 hPa in 25–50-hPa increments in the ERA5 and 50-hPa increments in the GFDL HiRAM and Zetac hurricane model simulations. However, only 850- and 500-hPa isosurfaces are used for GFDL HiFLOR due to limited data availability potentially yielding earlier transition times (Liu et al. 2017; Schenkel et al. 2018).

e. Rhines scale

We compare meridional variations in TC outer size from our simulations with a Rhines scaling to determine if TC outer size in future climates is consistent according to expectations from theory. The Rhines scale (L_β) is defined as (Rhines 1975; Chavas and Reed 2019)

$$L_\beta = \frac{\pi}{2}\sqrt{\frac{U_\beta}{\beta}}, \tag{2}$$

where the $\pi/2$ factor converts the Rhines scale to a vortex radius, U_β is a characteristic velocity scale for the broad outer circulation of the TC, and $\beta = df/dy = (2\Omega/a)\cos\phi$ is the meridional gradient of the Coriolis parameter, $\Omega = 7.292 \times 10^{-5}$ s^{-1} is the Earth's rotation rate, $a = 6371$ km is Earth's mean radius, and ϕ is the storm center latitude. We set the constant U_β to our TC outer size velocity of 8 m s^{-1}, similar to Chavas and Reed (2019).

We exclude the mean meridional relative vorticity gradient from the Rhines scale because it is generally much smaller than the meridional planetary vorticity gradient β over the open ocean, particularly in the lower troposphere. However, the ambient relative vorticity gradient may be occasionally large near strong lower-tropospheric jets, which may be significant during extratropical transition and motivate the exclusion of these cases. Hence, our analysis focuses on the simple definition of the Rhines scale given by Eq. (2).

The velocity scale U_β can be assumed constant because the radial structure of the quiescent TC outer circulation is itself relatively constant in space and time (Chavas and Lin 2016). It may also be held constant in a future climate because the physics of the outer wind field are well understood and depend only weakly on temperature for modern climate conditions (Chavas et al. 2015). As a result, the precise value of U_β is not important since it is a constant that does not alter the scaling properties of L_β. Note that the form of the constant $\pi/2$ factor in L_β is also somewhat arbitrary, suggesting that the output value from the equation should not be interpreted as an exact threshold (Chavas and Reed 2019). Rather, L_β should be considered as a scaling for qualitatively comparing TC outer size differences among different environments and climates. This interpretation is also consistent with the physics of the Rhines scale described above: It is not an absolute TC size scale but rather represents a process that acts to shrink larger TCs faster (Lu and Chavas 2022), thereby shifting the distribution of TC size toward smaller storms (Chavas and Reed 2019). We compare the meridional variation of L_β against the meridional variation of TC outer size. Moreover, L_β depends principally on β, which is thermodynamically invariant and hence is not expected to change significantly under climate change for comparison with our future climate simulations.

f. Statistical testing

In our analysis, we use bootstrap testing to determine whether control and future climate simulations are different from one another. The test provides a measure of whether any signal from anthropogenic warming is larger than internal variability noise for a given simulation. A 1000-sample bootstrap resampling with replacement for a two-tailed test is used to define whether the 5th, 25th, 50th, 75th, and 95th percentiles of the distribution are significantly different at the 10% and 5% level. For the radial and plan view plots, p values for each local null hypothesis are defined using a false discovery rate with values of 0.2 and 0.1, which approximately correspond to a global significance level of 10% and 5%, respectively (Benjamini and Hochberg 1995; Ventura et al. 2004; Wilks 2016). The false discovery rate conservatively requires smaller p values to reject the local null hypotheses. This more stringent standard reduces the false rejections of local null hypotheses associated with random fluctuations and strong spatial autocorrelation that yield false interpretation of results (Benjamini and Hochberg 1995; Ventura et al. 2004; Wilks 2016). For our bootstrap testing, the degrees of freedom are conservatively defined using the number of uniquely named TCs rather than the number of 6-h track points since outer size varies slowly over the storm life cycle (Merrill 1984; Weatherford and Gray 1988). Indeed, quantification of the effective degrees of freedom determined from the lag-1 autocorrelation (Bretherton et al. 1999) yields values similar to the number of TCs. In the interest of brevity, some of our results will only show the mean of the 10 CMIP3/A1B Zetac-downscaling GFDL hurricane simulation ensemble members. In these instances, our analysis will show when statistical testing indicates 80% of ensemble members agree on the sign of the result similar to prior work (Neelin et al. 2006; Pendergrass et al. 2017; Knutson et al. 2022).

3. Analysis and results

We first examine how TC outer size and structure change when considering all data and then focusing regionally in the North Atlantic. Next, we investigate outer size and structure changes during the North Atlantic TC life cycle with a focus on genesis and lifetime maximum r_8. Finally, we analyze the factors associated with these outer size and structure changes including differences in North Atlantic TC outer size growth rate, lifetime, and track changes.

a. Full lifetime

Most HiFLOR and GFDL hurricane model simulation projections suggest that North Atlantic TC outer size should remain unchanged, with no significant differences across the five statistics tested, as shown in box-and-whisker plots of r_8 data (Fig. 1). This result is consistent with Yamada et al. (2017). Moreover, the lack of change in the 95th percentile of r_8 is consistent with expectations from the Rhines scale. Specifically, median r_8 values in all control simulations range from 347 to 495 km versus from 375 to 520 km in the late twenty-first century. However, the Zetac CMIP3/A1B HadGEM1 shows statistical decreases in three statistics. In the HadGEM1 simulation, the magnitude of these reductions is marginally above the values associated with significance levels considered here (i.e., 10% level). Prior work has shown that the projection of strongly reduced TC frequency and intensity in the HadGEM1 simulation is an outlier among the Zetac CMIP3/A1B simulations (Knutson et al. 2013, 2022), which is consistent with the (outlier) TC outer size projections from HadGEM1 in the present study. The large reductions in TC frequency and intensity in the CMIP3/A1B HadGEM1 simulation were attributed to 1) increased thermodynamic stability associated with larger increases in tropical upper-tropospheric temperatures relative to the other downscaled ensemble members and 2) particularly strong shifts in TC genesis and tracks toward the northwest into climatologically less favorable environments closer to land (Knutson et al. 2013, 2022). Additionally, several simulations show either nonsignificant increases or decreases that fall just short of the significance threshold suggesting uncertainty in concluding that projected r_8 remains unchanged. In particular, the two simulations forced with repeating identical cycles of SSTs and radiation (i.e., HiFLOR and HiRAM) suggest small, nonsignificant increases in r_8, while the simulations containing present-day variability suggest either small decreases

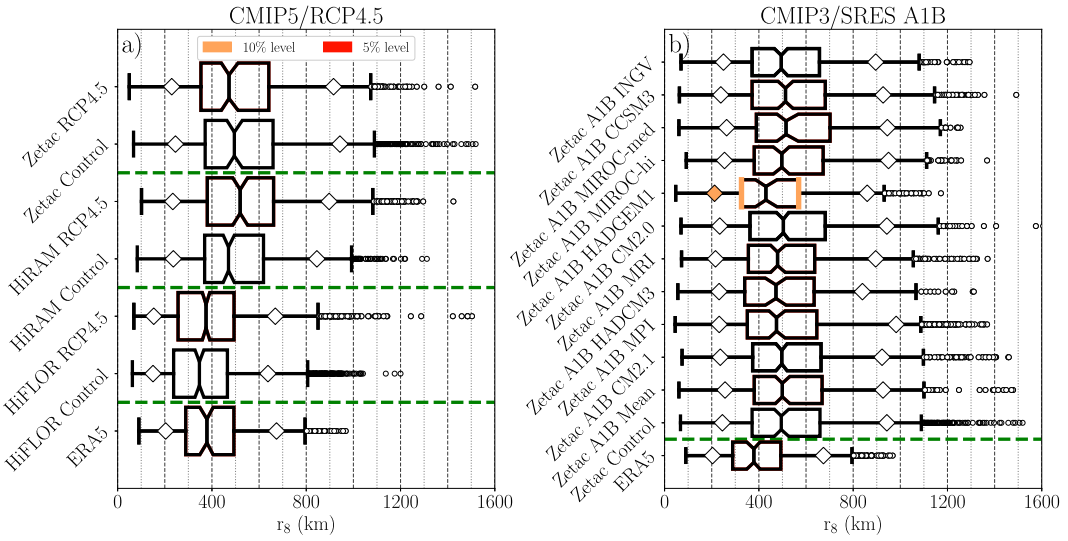

FIG. 1. Box-and-whisker plot of r_8 (km) for all 6-h North Atlantic TC times in the control and late-twenty-first-century simulations for the (a) CMIP5/RCP4.5 and (b) CMIP3/SRES A1B simulations. Each late-twenty-first-century simulation contains the corresponding control simulation within the same panel for ease of comparison. The box plots display the median (black vertical line near box center), the 95% confidence interval of the median calculated from a 1000-sample bootstrap approach with replacement (notches on boxes), the interquartile range (black box perimeter; $[q_1, q_3]$), the whiskers (black-capped lines), and the 5th and 95th percentiles (diamonds). The lower whisker is the first datum above $q_1 - 1.5(q_3 - q_1)$ and the upper whisker is the first datum below $q_3 + 1.5(q_3 - q_1)$. The following notation denotes when the future climate simulation is different from the current climate simulation for a given simulation: 1) thick colored middle line in the box for the median, 2) thick colored left and right sides of the box for the 25th and 75th percentiles, respectively, and 3) colored diamond for 5th and 95th percentiles. Light brown and red coloring denote statistics with significant differences between the current and future climate at the 10% and 5% levels, respectively. Horizontal dashed green lines denote groups of models within each climate change scenario. The reanalysis data are provided, but not statistically tested against the simulations in the interest of brevity. The reanalysis r_8 distribution is expected to be shifted toward smaller values than the GFDL hurricane model data due to the use of 35-m winds in the latter compared to 10-m winds in the former.

or nonsignificant increases (i.e., Zetac). This large variability in the Zetac-downscaling simulations may suggest that the ensemble members are exploring more of the uncertainty parameter space. The outlier CMIP3/A1B HadGEM1 simulation also suggests the importance of model boundary and initial conditions to our results. Last, a comparison of r_8 from HiFLOR and the GFDL hurricane model control simulations shows values that are comparable to the ERA5 providing confidence in these results, especially given the use of the lowest vertical level in the GFDL hurricane model (Knutson et al. 2015; Schenkel et al. 2018). Differences between r_8 in the ERA5 and simulations are not surprising for several reasons including differences in model configuration (e.g., use of 6-h data assimilation in reanalysis) and the simulation of dynamically consistent realizations of TC activity rather than any particular observed TC (Knutson et al. 2015; Hersbach et al. 2020).

Composite radial profiles of the azimuthal-mean near-surface azimuthal wind (Fig. 2) show that the above conclusions are not an artifact of using r_8. We show plots here of the mean of all 10 Zetac CMIP3/A1B ensemble simulations, excluding the mean simulation, here and elsewhere instead of showing each ensemble member. All four sets of late-twenty-first-century simulations show small differences in near-surface winds including median differences of -0.4–0.7 m s^{-1} in the TC outer region (i.e., radius $\geq$ 200 km) that fall short of significance thresholds. These results are also consistent with no change in azimuthal-mean rainfall in the outer region of North Atlantic TCs (Knutson et al. 2015; Lin et al. 2015; Yamada et al. 2017).

There are also generally no regional TC outer size differences in the North Atlantic basin between the current and late-twenty-first-century climate as shown using gridded maps of median r_8 (Fig. 3). The sample size of 6-h TC track points for the same grid is shown in Fig. S3 of the supplemental material. Both the ERA5 and control simulations show a positive meridional gradient in median r_8. This increase in median r_8 with latitude is broadly consistent with prior studies and the thermodynamically invariant Rhines scaling (Merrill 1984; Chavas and Reed 2019). Median differences between the present-day and future climate among simulations range between -130 and 253 km, which is not statistically different at any given grid point or in the zonal mean including those locations closest to land. More specifically, those simulations with repeating SST and radiative forcing (i.e., HiFLOR and HiRAM) show slightly larger TCs in most of the tropics and subtropics by the late twenty-first century. In contrast, simulations that include current climate variability (i.e., Zetac CMIP5/RCP4.5 and the mean of the CMIP3/A1B ensemble

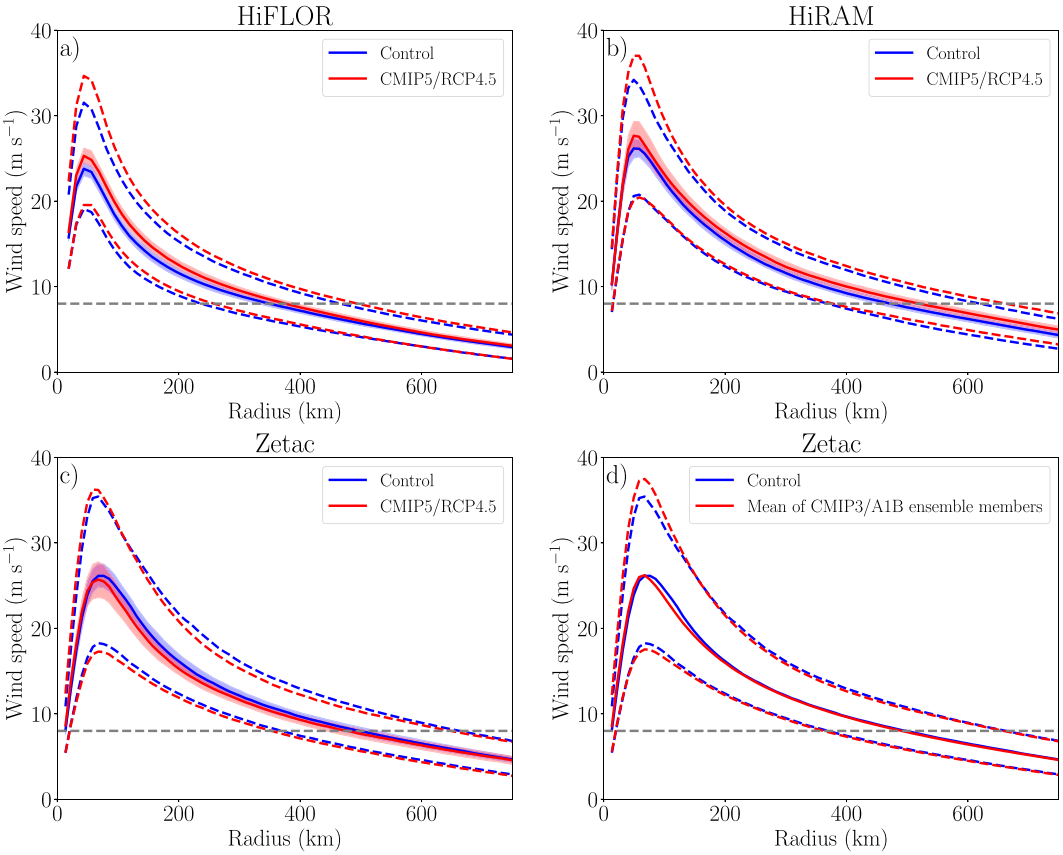

FIG. 2. Radial profile of composite median (solid line) with its 95% confidence interval (shaded) calculated using a 1000-sample bootstrap approach, and the interquartile (dashed lines) of the azimuthal-mean near-surface azimuthal wind (m s^{-1}) for the control, and late-twenty-first-century simulations in (a) HiFLOR, (b) HiRAM-downscaling, and (c) Zetac-downscaling from the CMIP5/RCP4.5 simulation, and (d) the mean of the Zetac-downscaling from the 10 CMIP3/A1B ensemble members (excluding the ensemble mean). None of the radii show significant differences in median values between the current and late-twenty-first-century climate for a false discovery rate of $\alpha = 0.1$ or $\alpha = 0.2$. In (d), ≥80% of the 10 Zetac-downscaling CMIP3/A1B ensemble members show no change in azimuthal wind speeds at all radii. HiFLOR wind speed data are at 10 m [in (a)], while the GFDL hurricane model simulation data are at the lowest model level (e.g., ~35 m).

members) show responses ranging from nonsignificant decreases to nonsignificant increases with spatial patterns that are less coherent among ensemble members, which may not be surprising given the variability in initial conditions among the CMIP3/A1B ensemble members.

Together, these HiFLOR and GFDL hurricane model simulations suggest that projected TC outer size and structure remain unchanged by the late twenty-first century. However, some uncertainty exists given that several simulations either show significant results or fall just short of these thresholds. The lack of differences shown here thus far agrees with prior modeling assessments (Yamada et al. 2017), the absence of decadal trends in both reanalyses and satellite-derived data from the satellite era (Knaff et al. 2014; Mok et al. 2018; Zhang and Chan 2022), and expectations from theory (Rhines scale; Rhines 1975; Chavas and Reed 2019). This analysis raises questions about whether stronger anthropogenic climate change scenarios (i.e., RCP8.5; Taylor et al. 2012) would yield larger differences with greater consistency in both the sign and spatial patterns among simulations. The absence of consistency among simulations with and without current climate variability may suggest that the climate change scenarios used here (e.g., CMIP5/RCP4.5 versus all CMIP3/A1B ensemble members) are a secondary factor influencing TC outer size compared to either model internal variability or current climate variability in the Zetac-downscaling simulations. Next, we consider if differences in r_8 occur at any point in the TC life cycle.

b. *Life cycle of TC outer size*

Differences between the life cycle of North Atlantic TC outer size in the present-day and future climate are shown in Fig. 4 for HiFLOR and GFDL hurricane model simulations. To facilitate the comparison of TCs with different lifespans, the life cycle of r_8 is shown as a fraction of the storm lifetime. Each simulation suggests a steady increase in r_8 through the four quartiles of the TC life cycle similar to prior work for the

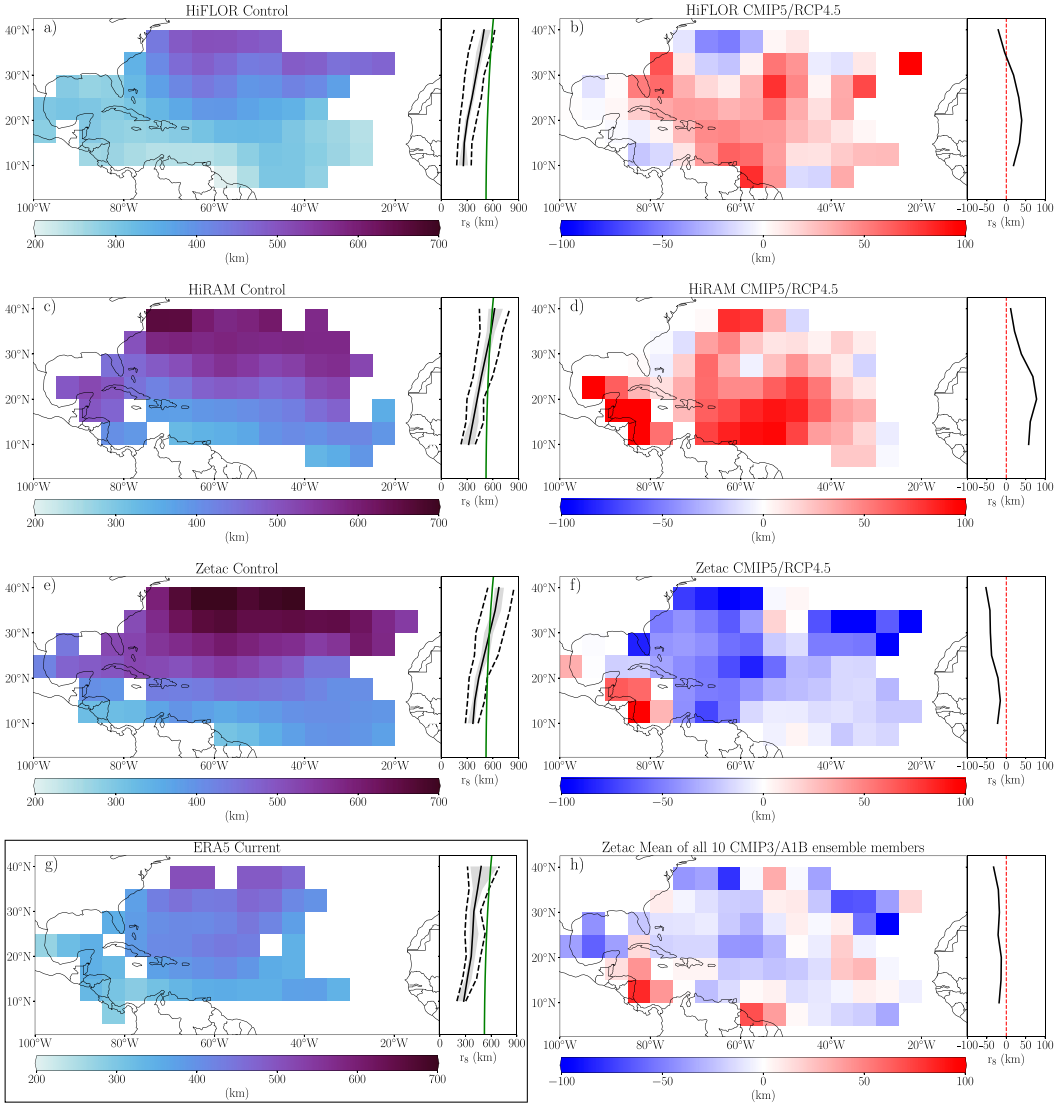

FIG. 3. Plan view of composite median r_8 (km) in the control and its difference with the future climate on a 5° × 5° grid (shown in left plots) in (a),(b) HiFLOR, (c),(d) HiRAM-downscaling, (e),(f),(h) Zetac-downscaling simulations, and (g) ERA5, where (a), (c), (e), and (g) are for the current climate (control) and (b), (d), (f), and (h) are for the late twenty-first century minus the control. The right panels show the zonal median (black line) and its 95% confidence interval (gray shading), and the interquartile range (black dashed lines) of r_8 for the current climate in (a), (c), (e), and (g) whereas (b), (d), (f), and (h) show the difference between median values. The black rectangle around the ERA5 panel is used to distinguish it from the rest of the simulations. The green line in the side plots of (a), (c), (e), and (g) shows the Rhines scaling for r_8 vs latitude. There must be ≥10 values from ≥3 unique TCs for a median value to be given for a grid box. The two-dimensional grid is smoothed once with a 9-point smoother, while the side panel is smoothed once with a 3-point smoother. None of the grid boxes show significant differences in median values between the current and late twenty-first-century climate for a false discovery rate of $\alpha = 0.1$ or $\alpha = 0.2$. In (h), ≥80% of the 10 Zetac-downscaling CMIP3/A1B ensemble members show no significant changes in r_8 at each grid point or in the zonal mean.

North Atlantic (Schenkel et al. 2018). A comparison of control and future climate simulations without current climate variability shows that r_8 changes often become increasingly larger later in life especially in the late twenty-first century, although none of the median differences among the simulations are statistically different. Nonetheless, there is no consistency among those simulations on when these differences begin during the TC life cycle. In particular, HiFLOR shows marginally larger TCs in the control simulation in the first quartile, followed by the CMIP5/RCP4.5 simulations becoming larger throughout the rest of the TC lifetime, whereas HIRAM shows CMIP5/RCP4.5 simulations with larger TCs with greater differences as storm age increases. In contrast, the Zetac-downscaled simulations have no consistent patterns with age.

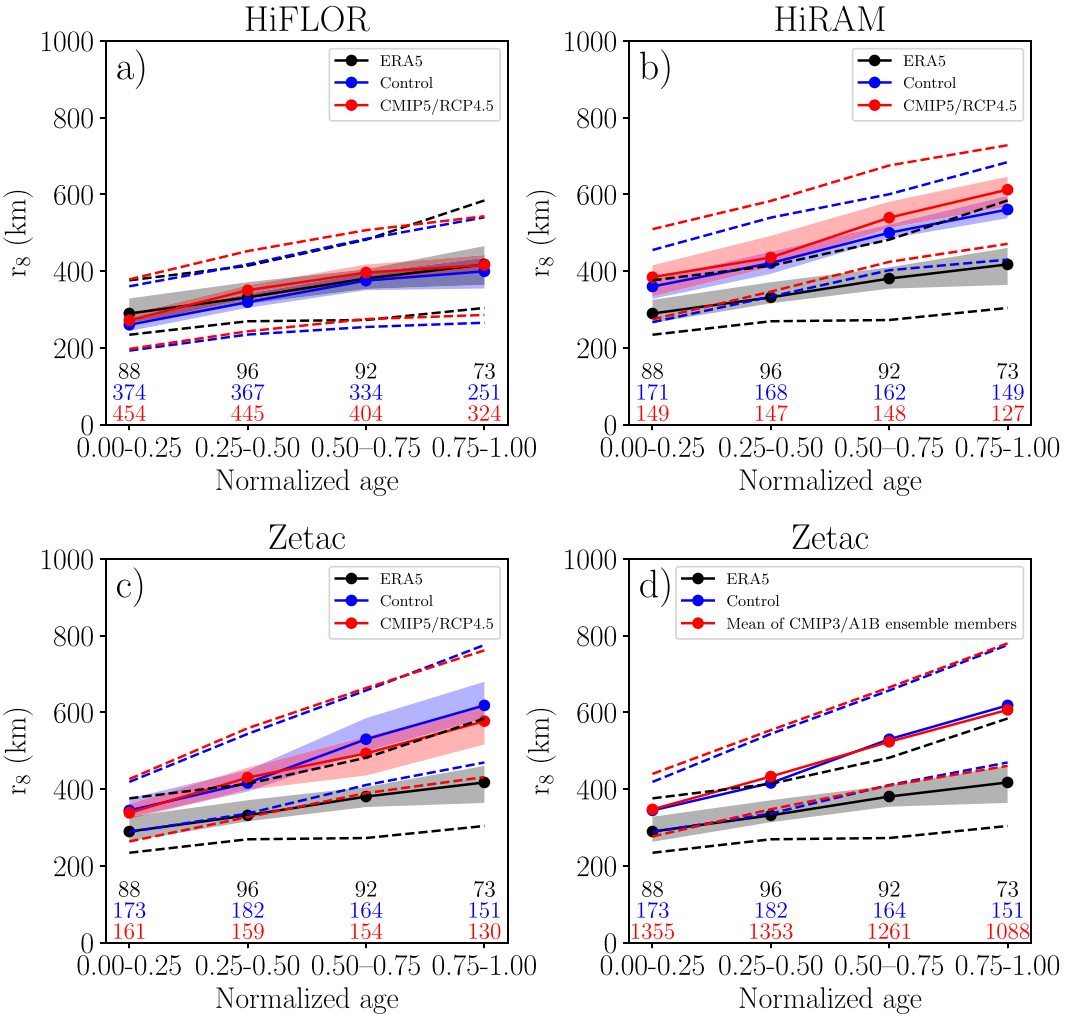

FIG. 4. Composite time series of median (solid line) and its 95% confidence interval (shaded) calculated using a 1000-sample bootstrap approach, and the interquartile range (dashed lines) of r_8 (km) for the control, and late-twenty-first-century simulations in (a) HiFLOR, (b) HiRAM-downscaling, (c) Zetac-downscaling CMIP5/RCP4.5, and (d) the mean of the Zetac-downscaling of all 10 CMIP3/A1B ensemble members (excluding the ensemble-mean simulation). The normalized age coordinate is computed by taking the age of each TC and dividing it by its lifetime to compare storms with varying lifespans. The r_8 data are then averaged within each quartile for a given TC before computing the median and its 95% confidence interval, and the interquartile range following Schenkel et al. (2018). The numbers provide the sample sizes for each simulation and bin. None of the simulations show r_8 values that are statistically different between the present-day and future climate according to p values defined using a false discovery rate of $\alpha = 0.1$ or $\alpha = 0.2$. In (d), ≥80% of the 10 Zetac-downscaling CMIP3/A1B ensemble members show no significant changes in r_8 throughout the normalized TC lifetime.

Next, we examine r_8 at specific milestones in the TC life cycle beginning with genesis. Projected genesis r_8 does not change between the current and late-twenty-first-century climate (Fig. 5). Compared to all 6-h times (Fig. 1), the r_8 distribution at genesis is narrower (Schenkel et al. 2018). However, the differences in genesis r_8 between the control and late-twenty-first-century simulations are typically smaller in magnitude compared to all 6-h time results for most simulations. Specifically, median r_8 is 219–341 km in the control versus 213–359 km in the late twenty-first century among all simulations. None of the simulations show significant differences in genesis outer size by the late twenty-first century among any of the statistics examined. This provides further support that any changes that do occur in outer size likely arise later in the TC life cycle. We also show projected changes in TC genesis latitude (Fig. 6) given that the Rhines scaling suggests larger outer sizes at poleward latitudes (Chavas and Reed 2019; Lu and Chavas 2022). The majority of simulations show no change in TC genesis latitude. While several simulations show changes in one or more distribution statistics, these changes are inconsistent ranging from small equatorward shifts to large poleward shifts. More importantly, these shifts

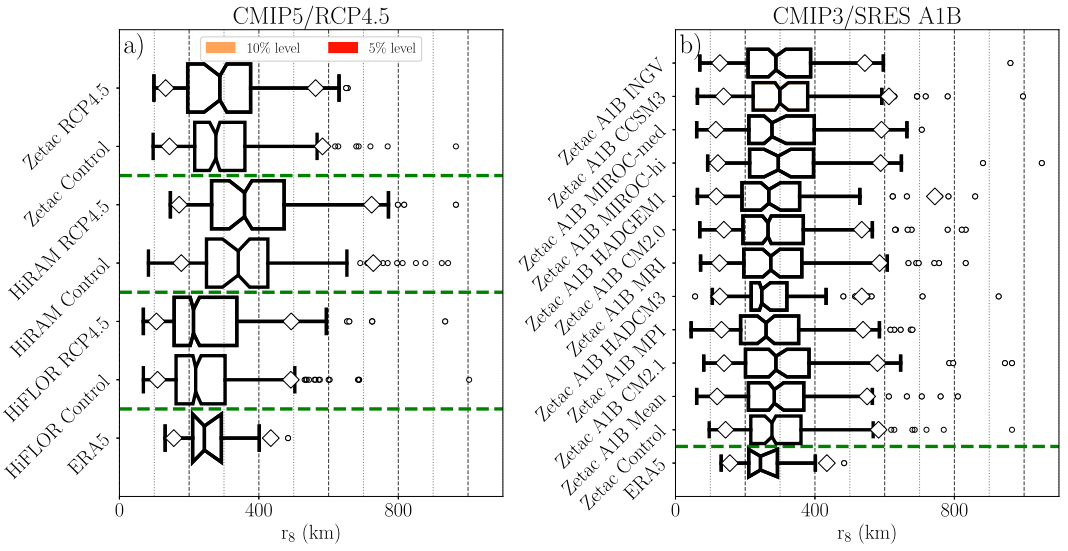

FIG. 5. As in Fig. 1, but for genesis r_8 (km).

in genesis latitude are not associated with changes in TC outer size in the simulations.

Composite radial profiles of near-surface azimuthal winds at TC genesis also typically do not change by the late-twenty-first-century climate (Fig. 7). Compared to Fig. 2, the distribution of near-surface winds is much narrower at all radii and there is a greater overlap between control and late-twenty-first-century simulations among HiFLOR and GFDL hurricane model simulations. Specifically, median differences range between −0.7 and 0.7 m s^{-1} in the TC outer region, which are not significantly different from one another. Moreover, the largest differences tend to be concentrated in the TC inner core with smaller, nonsignificant differences outside these radii.

We next examine lifetime maximum outer size, which occurs in the latter portions of the TC life cycle (Merrill 1984; Schenkel et al. 2018). Compared to genesis outer size, the distribution of lifetime maximum r_8 (Fig. 8) is broader in both the control and future simulations (Schenkel et al. 2018). Similar to all 6-h data and at genesis, lifetime maximum r_8 typically also remains unchanged by the late twenty-first century among nearly all HiFLOR and GFDL hurricane model simulations. The lack of systematic changes in any tested statistics in lifetime maximum r_8 is similar to the results given by the Rhines scale (Chavas and Reed 2019). The differences between lifetime maximum r_8 among the control and future simulations are similar, but slightly larger, compared to those for all r_8 data (Fig. 1). In particular, median values of lifetime maximum r_8 range from 422 to 663 km in the control versus from 456 to 666 km in the future climate among all simulations. Similar to Fig. 1, the Zetac CMIP3/A1B HadGEM1

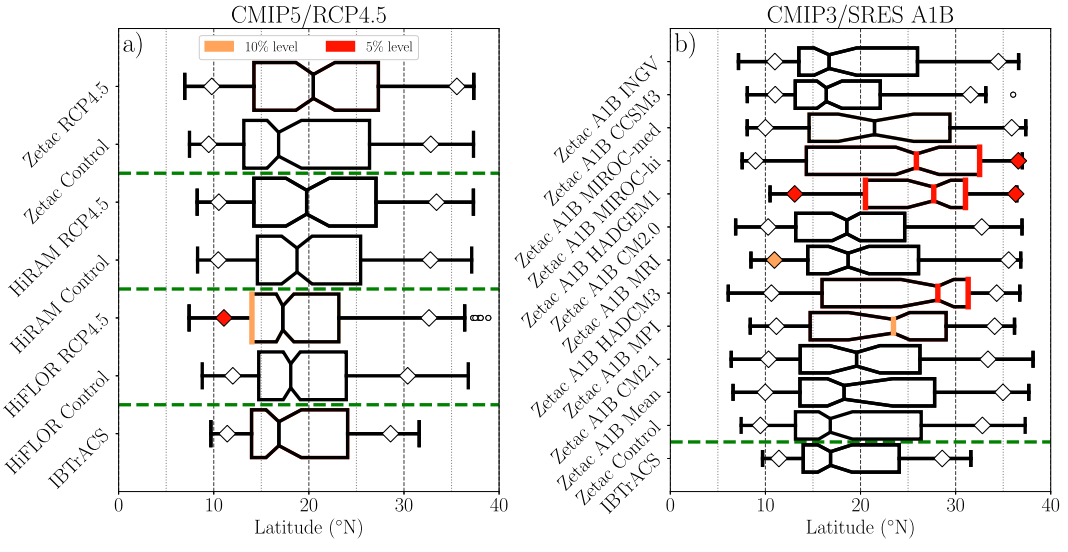

FIG. 6. As in Fig. 1, but for genesis latitude (°N).

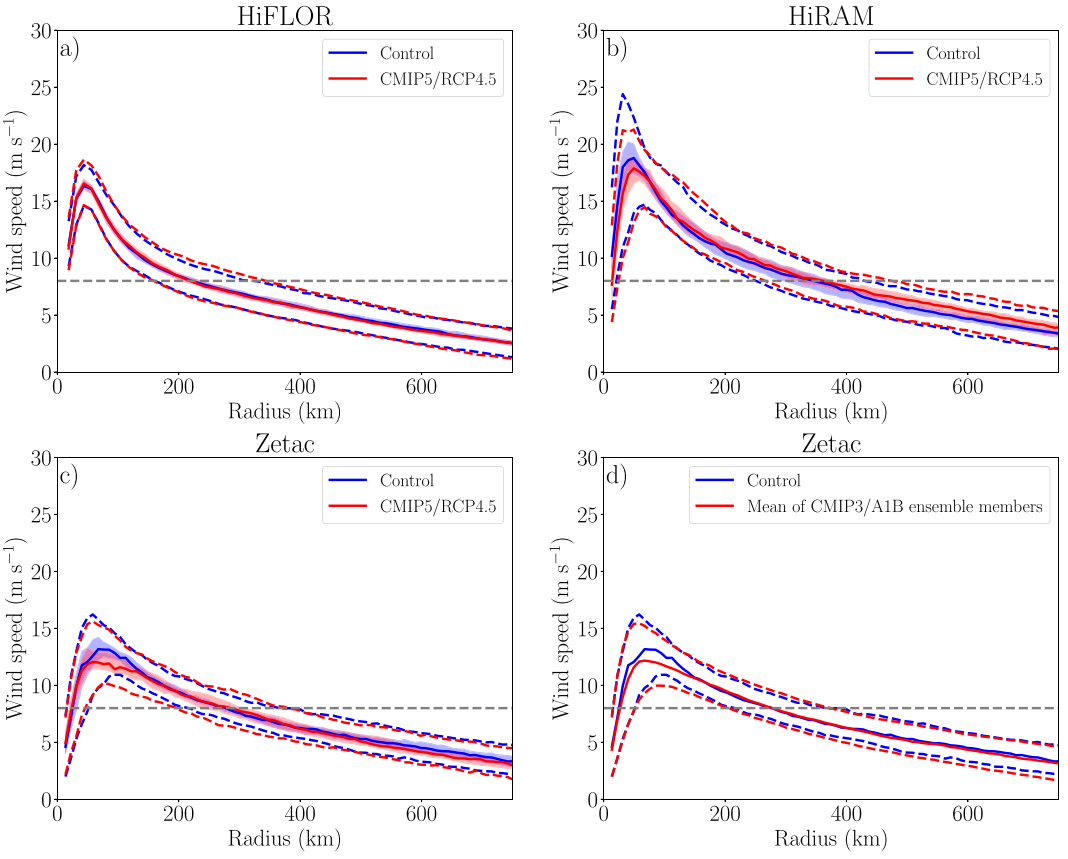

FIG. 7. As in Fig. 2, but at genesis (m s^{-1}). In (d), ≥80% of the 10 Zetac-downscaling CMIP3/A1B ensemble members show no change in azimuthal wind speeds at all radii.

simulation shows significantly smaller r_8 in two statistics by the late twenty-first century. Several simulations show differences that just miss the significance threshold. However, there remains disagreement among the simulations on the sign of these nonsignificant changes in TC outer size. Similar to all 6-h data, HiRAM and HiFLOR suggest nonsignificant increases, whereas the Zetac simulations show a range of possibilities from significant decreases to nonsignificant increases.

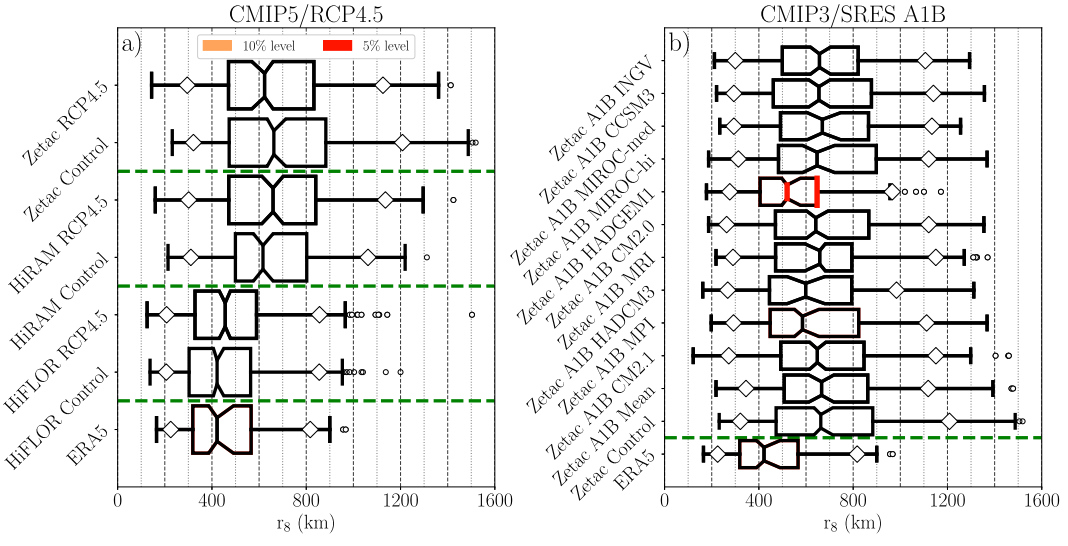

FIG. 8. As in Fig. 1, but for lifetime maximum r_8 (km).

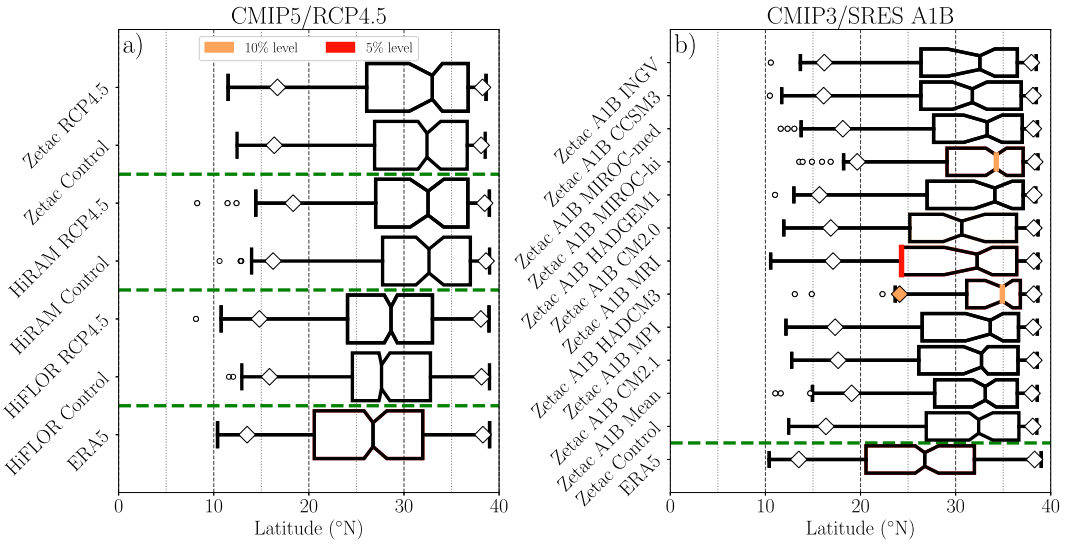

FIG. 9. As in Fig. 1, but for the latitude of lifetime maximum r_8 (°N).

We also show projected changes in the latitude of lifetime maximum r_8 in Fig. 9, which is important from a risk perspective (Lin et al. 2014, 2015) as well as for trying to wholly understand the lifetime maximum r_8 results in the context of the Rhines scaling (Chavas and Reed 2019). Only three of the Zetac-downscaling simulations show changes in at least one statistic in the lifetime maximum r_8 distributions, while HiRAM and HiFLOR simulations show no differences. Moreover, the sign of these changes is inconsistent ranging from a poleward shift in 1–2 statistics from the CMIP3/A1B HADCM3 and MIROC-hi simulations to an equatorward shift in the lower quartile of the CMIP3/A1B MRI simulation. The absence of stronger, systematic changes in both the magnitude and latitude of lifetime maximum r_8 is consistent with expectations from the Rhines scaling (Chavas and Reed 2019).

Composite radial profiles of near-surface azimuthal winds during lifetime maximum outer size also do not show significant changes between the control and future climates in most simulations (Fig. 10). Specifically, differences between outer region winds in the control and late twenty-first-century range between -1.3 and 1.1 m s^{-1}, which is larger than the profiles for all 6-h times (Fig. 2) or genesis (Fig. 7). The largest differences are concentrated near the radius of maximum winds with much smaller, nonsignificant differences outside the TC inner core among nearly all simulations.

These results suggest that outer size and structure likely remain unchanged through the TC life cycle by the late twenty-first century in HiFLOR and the GFDL hurricane model simulations. In particular, the lack of change in lifetime maximum r_8 shown here and as predicted by the Rhines scale increases the confidence in our results. However, the absence of complete consensus among simulations suggests some uncertainty especially in the latter portion of the lifetime when maximum outer size typically occurs. The lack of differences at genesis may partially explain why lifetime maximum TC outer size often remains unchanged in most HiFLOR and GFDL hurricane model simulations given the strong association between initial outer size and subsequent growth rates (Schenkel et al. 2018; Martinez et al. 2020). Moreover, this analysis may suggest that the outer size of TC precursor disturbances does not change by the late twenty-first century given its association with genesis TC outer size (Rotunno and Emanuel 1987; Cocks and Gray 2002; Lee et al. 2010). Finally, the results from most simulations are consistent with expectations of relatively constant maximum outer size with warming from the Rhines scaling, which instills greater confidence in our conclusions. Next, our analysis examines the factors associated with changes in TC outer size in certain simulations between the current and late twenty-first century.

c. *Factors associated with outer size differences*

We first investigate whether TC outer size growth rates remain unchanged by the late twenty-first century as shown in Fig. 11 in HiFLOR and the GFDL hurricane model simulations. Both the control and future climate TC growth rates are skewed toward positive values consistent with growth (Merrill 1984; Schenkel et al. 2018). Moreover, the HiFLOR and GFDL hurricane model growth rates tend to be statistically larger than those in the ERA5. Median values range from 19 to 41 km day^{-1} in the control to 19–50 km day^{-1} in the late twenty-first century. The difference between these ranges in the control and future simulations is not significant among most HiFLOR and GFDL hurricane model simulations, although some are just shy of being statistically different. Only the Zetac CMIP3/A1B CM2.0 simulation shows significant increases in daily growth rates for the 25th percentile by the late twenty-first century, yet no significant changes in its r_8 distribution (Fig. 1). In contrast, the Zetac CMIP3/A1B HadGEM1 simulation showed significant decreases in the 95th percentile. The decreased growth rates within Zetac CMIP3/A1B HadGEM1 may be due to the increased upper-tropospheric

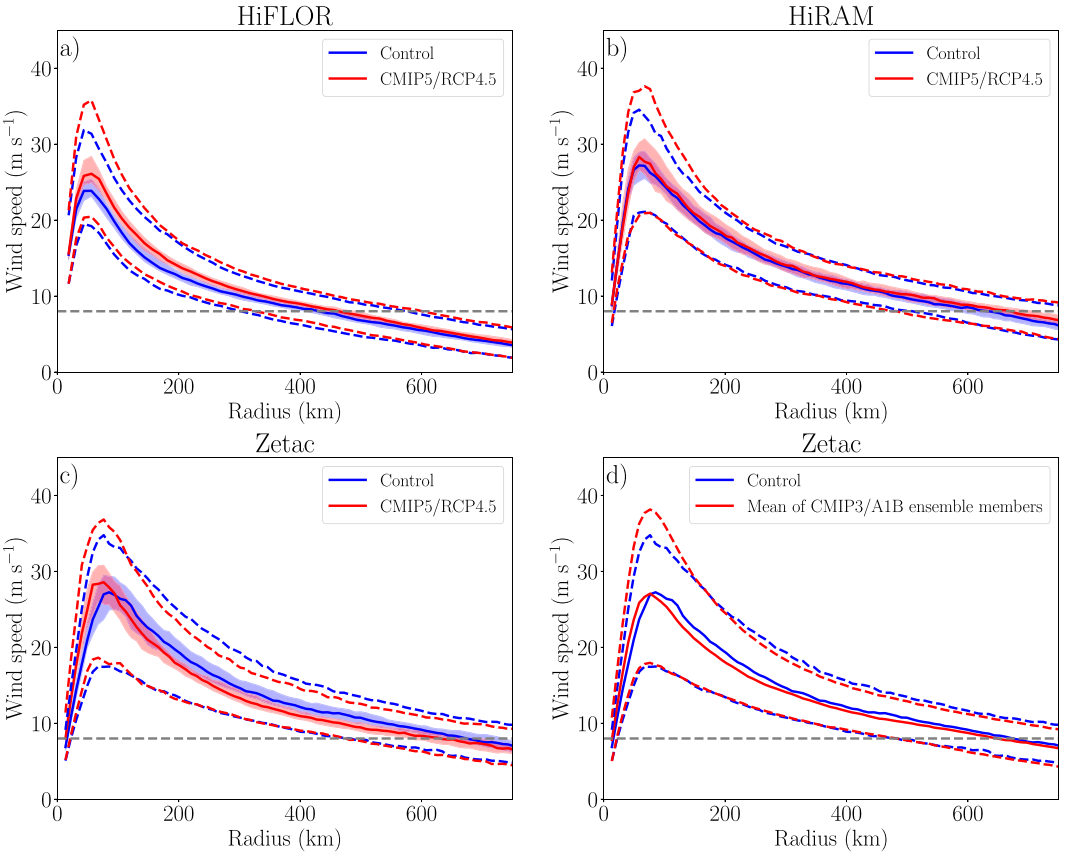

FIG. 10. As in Fig. 2, but at lifetime maximum r_8 (m s^{-1}). In (d), ≥80% of the 10 Zetac-downscaling CMIP3/A1B ensemble members show no change in azimuthal wind speeds at all radii.

warming that is associated with a northwestward shift in TC genesis and tracks and, more broadly, less favorable conditions for TC genesis and intensification (Knutson et al. 2013, 2022). More generally, these small, often nonsignificant changes in growth rates suggest that other factors may be responsible for the outer size decreases in these Zetac CMIP3/A1B HadGEM1 simulation.

Next, our analysis examines differences in TC lifetime between the current and late-twenty-first-century climate as

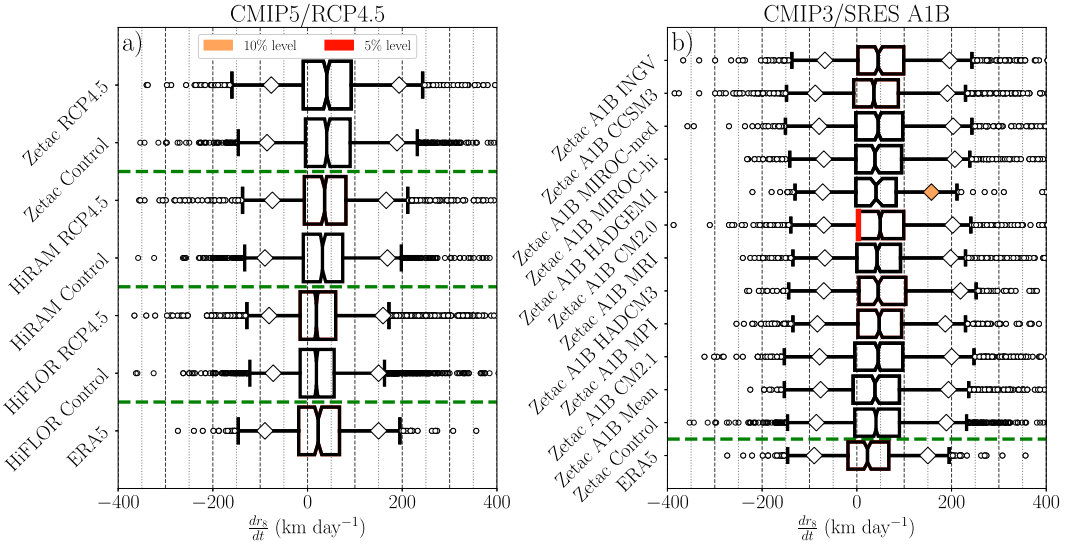

FIG. 11. As in Fig. 1, but for dr_8/dt (km day^{-1}).

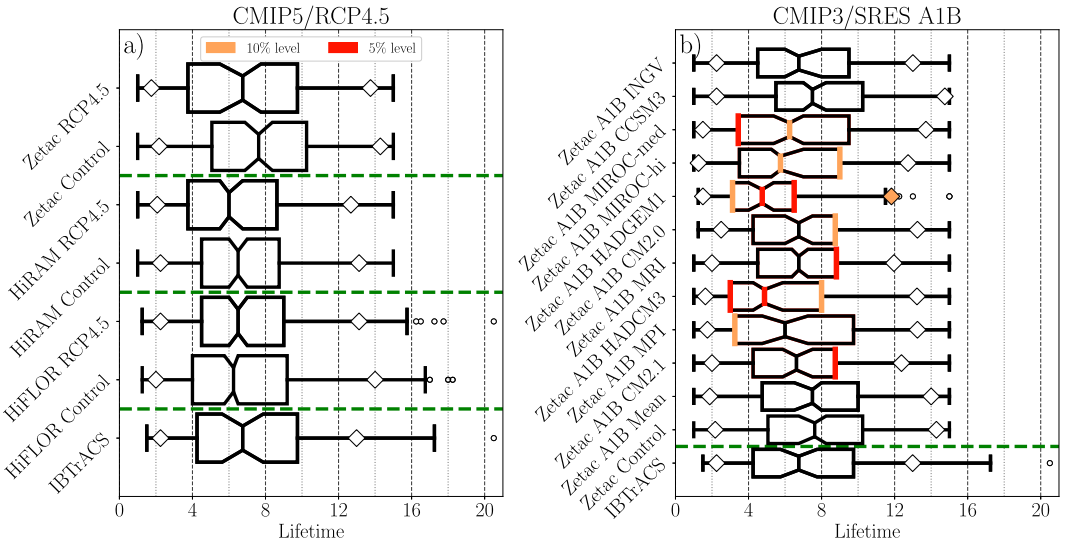

FIG. 12. As in Fig. 1, but for TC lifetime (days).

shown in Fig. 12. The lifetime is examined given the association between long TC lifetime and larger outer size that exists due to the slow growth of outer size in the North Atlantic (Merrill 1984; Schenkel et al. 2018). The 39°N latitude threshold used for the GFDL simulation northern boundary may limit our ability to characterize the full life cycle of all TCs. However, most TCs in the current and late twenty-first century begin extratropical transition starting at this northern boundary (Liu et al. 2017; Michaelis and Lackmann 2019). The simulations show greater differences in TC lifetime compared to any of the outer size and structure parameters examined here. While the HiRAM-downscaling and HiFLOR simulations show no significant changes in TC lifetime, the majority of Zetac-downscaling ensemble members show significant decreases in anywhere between 1 and 4 tested distribution statistics. Specifically, the median lifetime in the Zetac-downscaling simulations with significant decreases ranges from 4.8 to 6.6 days in the late twenty-first century compared to 7.6 days in the control simulations. The shorter TC lifetimes in these simulations may be associated with a northwestward shift in both TC genesis and tracks toward the continental United States yielding decreased time before landfall and closer proximity to midlatitude baroclinic environments that either yield cyclolysis or extratropical transition (Hart and Evans 2001; Liu et al. 2017). Moreover, the Zetac A1B HadGEM1 simulation, which is characterized by the strongest decreases in TC lifetime and r_8, shows less favorable conditions for TC intensification in the tropics in association with very pronounced upper-tropospheric warming (Knutson et al. 2013, 2022). In particular, the smaller r_8 values for the Zetac CMIP3/A1B HadGEM1 simulation (e.g., Fig. 1) appear to be associated with sharp reductions in TC lifetime and, to a lesser extent, outer size growth rates (Fig. 11). The remaining Zetac simulations with shorter TC lifetimes are not associated with smaller r_8. This result may be due to the following: 1) the greater, nonsignificant r_8 growth rate offsetting the TC lifetime decreases (e.g., Zetac CMIP3/A1B CM2.1) or 2) the decreases in storm lifetime not being of sufficient magnitude to be associated with r_8 decreases. Last, a large number of simulations show shorter TC lifetimes than the best track which are associated with shifts in TC tracks shown next.

The simulations with no changes in TC lifetimes also typically show small TC track changes between the current and late twenty-first century (Fig. 13). Specifically, the simulations with repeating identical cycles of SSTs and radiation (i.e., HiFLOR and HiRAM) show small, spatially incoherent track changes. However, the simulations with present-day climate variability (i.e., Zetac CMIP5/RCP4.5 and mean of the Zetac CMIP3/A1B ensemble simulations) show a northwestward shift toward the continental United States associated with an increased proportion of landfalling TCs (Knutson et al. 2022). This westward shift in TC tracks is also associated with a westward shift in TC genesis toward the continental United States in most Zetac-downscaling simulations [i.e., Fig. 7 from Knutson et al. (2022)]. Figure 8 from Knutson et al. (2022) also showed that the majority of the Zetac-downscaling simulations, including the CMIP/RCP4.5 simulation, project 1) stronger trade wind easterlies advecting TCs more quickly across the eastern and central Atlantic and 2) weaker midlatitude westerlies and, hence, farther westward propagation before TC recurvature. The reduction in midlatitude westerlies is also likely associated with a reduction in vertical wind shear, providing more favorable conditions for TCs in the midlatitudes (Knutson et al. 2022, 2013; Ting et al. 2019). Simulations that show significant reductions in TC lifetime (e.g., Zetac/A1B HadGEM1, HADCM3) show tracks more strongly shifted north and west. This shift in tracks and associated reduction in TC lifetime suggest less time for outer size growth before 1) cyclolysis associated with landfall (Knutson et al. 2022) or 2) cyclolysis or extratropical transition associated with midlatitude baroclinic environments (Hart and Evans 2001; Liu et al. 2017). Finally, the reductions in both TC outer size growth rates and lifetime

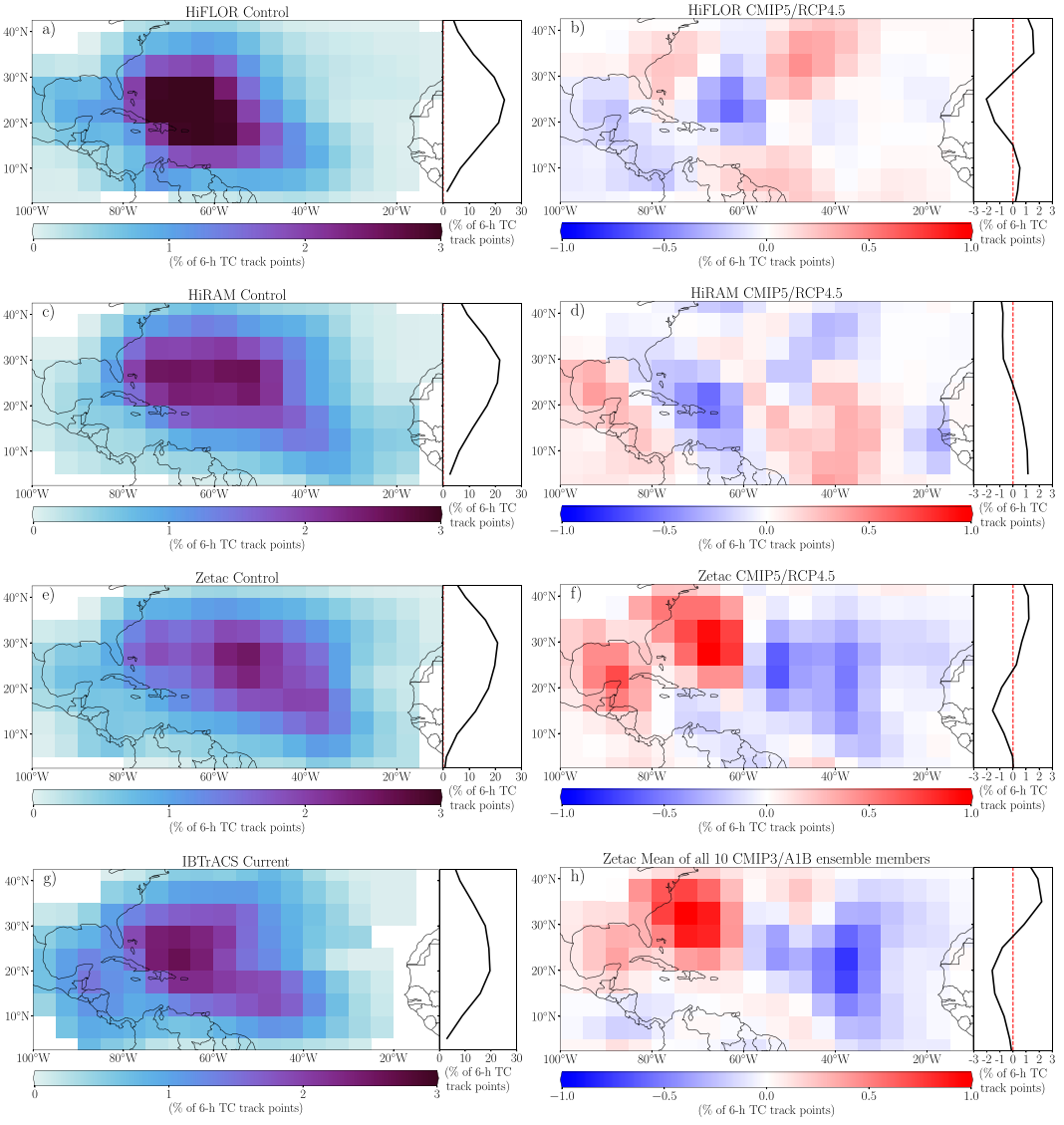

FIG. 13. Plan view of percentage of total 6-h TC track points in the current climate and its difference with the late-twenty-first-century climate on a 5° × 5° grid (left plots) in (a),(b) HiFLOR, (c),(d) the HiRAM-downscaling simulation, (e),(f),(h) the Zetac-downscaling simulations, and (g) ERA5, where (a), (c), (e), and (g) are for the current climate and (b), (d), (f), and (h) are for the late twenty-first century minus the current climate. The right plot shows the zonal median (black line) in (a), (c), (e), and (g), whereas (b), (d), (f), and (h) only show the difference between median values. The black rectangle around the ERA5 panel is used to distinguish it from the rest of the simulations. The two-dimensional grid is smoothed once with a nine-point smoother, while the side plot is smoothed once with a three-point smoother.

in Zetac/A1B HadGEM1 simulations may be associated with less favorable conditions for TC genesis and environments favoring weaker TC intensities (Knutson et al. 2013, 2022).

This section suggests that projected r_8 growth rates likely remain unchanged by the late twenty-first century, while a small number of Zetac-downscaling GFDL hurricane model simulations may show decreased TC lifetimes in association with a northwestward shift in tracks toward the continental United States. However, these storm lifetime changes do not appear to be associated with differences in r_8 between the control and late twenty-first century in most simulations. The lack of changes in r_8 growth rates in most simulations by the late twenty-first century may further suggest that the storm environments or precursor disturbance sizes are not substantially different given the previously identified importance of these factors (e.g., ambient relative humidity; Hill and Lackmann 2009; Knaff et al. 2017; Martinez et al. 2020).

4. Summary and discussion

The present study investigated whether projected North Atlantic TC outer size and structure change by the late

twenty-first century due to anthropogenic warming. We computed previously used TC outer size [i.e., the radius at which the azimuthal-mean near-surface azimuthal wind is less than or equal to 8 m s^{-1} (r_8)] and structure metrics (i.e., azimuthal-mean near-surface azimuthal wind) from three sets of TC-resolving simulations for the current (control) and late-twenty-first-century climate. These simulations were conducted with climate change scenarios using models from two different generations of CMIP experiments (SRES A1B and RCP4.5) and two different emission scenarios—CMIP3/A1B and CMIP5/RCP4.5. Our analysis focused on examining differences in North Atlantic TC outer size and structure for all 6-h times between the present day and the late twenty-first century, and regional variations in these differences. We also examined how the life cycle evolution of North Atlantic TC outer size and structure may change and the factors associated with these changes.

Our results suggest that the projected North Atlantic TC outer size and structure remain unchanged by the late twenty-first century in most HiFLOR and GFDL hurricane model simulations in agreement with predictions from the Rhines scaling. This outcome from real-Earth simulations is consistent with the lack of change in storm size with warming found in aquaplanet experiments with uniform global SSTs (Stansfield and Reed 2021). Nonetheless, this conclusion contains nontrivial uncertainty given that some simulations either showed limited changes in some statistics or fell just short of significance thresholds. Those limited small differences that occurred were exclusively associated with the Zetac-downscaling CMIP3/A1B HadGEM1 simulation, which has been previously shown to be a strong outlier for simulating TC activity compared to other ensemble members. More broadly, the Zetac-downscaling simulations yielded a range of solutions between significant decreases and nonsignificant increases. This variability may reflect the variety of initial conditions from the CMIP3/A1B ensemble, which allows these simulations to quantify more of the uncertainty parameter space. In contrast, those simulations forced with repeating identical cycles of radiation and SSTs showed nonsignificant r_8 increases. More specifically, our results showed that the TC outer size ranges between ~350 and 520 km in the current and future climate when considering all data. The HiFLOR and GFDL hurricane model simulations do not show any regional changes in North Atlantic TC outer size between the present-day and future climate. These results for outer size are consistent with the outer azimuthal-mean near-surface azimuthal wind field, which also remains unchanged.

This study also examined potential changes in outer size and structure during the North Atlantic TC life cycle. Our analysis showed that control and late-twenty-first-century TCs tended to be larger later in their life cycle, but no differences existed in outer size at any point during the TC lifetime. Closer examination of outer size and structure at genesis also showed smaller differences between the control and future simulations compared to all 6-h times. Consistent with expectations from the Rhines scale, lifetime maximum r_8 and its associated outer structure also do not show significant differences by the late twenty-first century in most simulations. However, the lifetime maximum r_8 results did fall just short of significance thresholds in HiFLOR and several GFDL hurricane model simulations.

Analysis of factors potentially associated with North Atlantic TC outer size and structure changes suggested no changes in outer size growth rates from the present-day to future climates in most simulations. TC lifetime also showed no changes in most simulations, although a large number of Zetac CMIP3/A1B simulations showed significant decreases in lifespans in association with a northwestward shift in TC tracks toward the continental United States by the late twenty-first century. However, HiFLOR and most GFDL hurricane model simulations showed small or inconsistent TC track changes by the late twenty-first century. The Zetac downscaling CMIP3/A1B HadGEM1 simulation was the only model showing large outer size differences, which were associated with a reduction in outer size growth rates and, more strongly, with lifetime. However, this model has been previously identified as an outlier among the Zetac simulations, which also suggests the importance of model initial and boundary conditions to our results.

In summary, these results suggest that the projected late-twenty-first-century North Atlantic TC outer size and structure likely remain unchanged in the future climate regardless of the phase of TC lifetime or region of the basin considered. Our analysis also addresses the motivating questions raised in the introduction:

1) Is there a consensus among multiple models on whether projected TC outer size and structure change between the current and late-twenty-first-century climate in the North Atlantic?
   Yes, there is consensus among multiple models suggesting that projected TC outer size and structure will remain unchanged by the late twenty-first century.
2) Are changes in TC outer size and structure confined to certain portions of the TC life cycle?
   No, TC outer size and structure are projected to be unchanged throughout the TC life cycle.
3) Do changes in TC outer size and structure occur only in certain regions of the North Atlantic?
   No, our simulations project no localized differences in TC outer size and structure in the North Atlantic between the current and late-twenty-first century climates.

These results suggest that any changes to North Atlantic TC outer size induced by anthropogenic warming are likely smaller than internal variability noise given the statistical testing results. These results also suggest that North Atlantic TC outer size differences are smaller than uncertainties introduced by differences in model configuration (e.g., downscaling) given the agreement among the simulations. The absence of projected changes in TC outer size is notable given the differences in TC genesis location, track, and intensity by the late twenty-first century in these simulations.

Together, these projections are consistent with reanalysis and satellite-derived trends from the last several decades and recent theory on what limits TC outer size as provided by the Rhines scaling, which instills greater confidence in our analysis. Our work provides crucial guidance to hazard and risk

modeling given the sensitivity of hazards to TC outer size and structure (Lin et al. 2014; Lu et al. 2018). Moreover, this study provides greater confidence in prior hazard studies, which have assumed that North Atlantic TC outer size and structure remain unchanged in the absence of a comprehensive multimodel assessment (Lin et al. 2015; Marsooli et al. 2019; Gori et al. 2022). Future work should quantify the sensitivity of North Atlantic TC outer size and structure to more extreme warming scenarios (e.g., CMIP5/RCP8.5) given that several simulations just missed exceeding the statistical thresholds under these less aggressive anthropogenic climate change scenarios. Moreover, a companion analysis should identify which environmental factors are responsible for no changes in TC outer size to provide a greater physical understanding of these results and their sensitivity to different climate warming scenarios. An additional future study should also examine how changes to internal climate variability by the late twenty-first century could alter TC outer size. The sensitivity of these results to the initial and boundary conditions and how they are imposed (e.g., uncoupled versus coupled SSTs, use of spectral nudging) should also be quantified and compared to variability associated with ensemble member spread. Finally, future work would benefit from projections run using a state-of-the-art regional hurricane model like the Hurricane Analysis and Forecast System (HAFS; Hazelton et al. 2021, 2022) or the Hurricane Weather Research and Forecasting model (HWRF; Gopalakrishnan et al. 2011, 2013).

Acknowledgments. This study is generously supported by NSF Grants 1520683 and 1652448 and the University of Oklahoma. The statements, findings, conclusions, and recommendations herein are those of the authors and do not necessarily reflect the views of the NSF and the University of Oklahoma. The authors are indebted to Joe Sirutis (GFDL) and Maofeng Liu (Princeton) for their help with the model simulations during the early stages of this project. The authors thank Michael Oppenheimer (Princeton), John Knaff (NOAA/NESDIS), Hiroyuki Murakami (GFDL), Kristin Calhoun (NSSL), Morris Bender (GFDL), Naoko Sakaeda (OU), Tim Marchok (GFDL), Robert Tuleya (GFDL), Jonathan Martinez (NCAR), and Chia-Ying Lee (Columbia) for insightful conversations. We would also like to thank Pang-chi Hsu (University of Hawaii) for guidance and input during the review process.

Data availability statement. ERA5 data are available through the NCAR RDA website (https://rda.ucar.edu/datasets/ds633.0/). IBTrACS data are available through the NCDC website (https://www.ncei.noaa.gov/data/international-best-track-archive-for-climate-stewardship-ibtracs/v04r00/access/netcdf/). The GFDL hurricane model track data used in this study are available upon request from the first author.

REFERENCES

Bender, M. A., I. Ginis, R. Tuleya, B. Thomas, and T. Marchok, 2007: The operational GFDL coupled hurricane–ocean prediction system and a summary of its performance. *Mon. Wea. Rev.*, **135**, 3965–3989, https://doi.org/10.1175/2007MWR2032.1.

Benjamini, Y., and Y. Hochberg, 1995: Controlling the false discovery rate: A practical and powerful approach to multiple testing. *J. Roy. Stat. Soc.*, **57**, 289–300, https://doi.org/10.1111/j.2517-6161.1995.tb02031.x.

Bhatia, K., G. Vecchi, H. Murakami, S. Underwood, and J. Kossin, 2018: Projected response of tropical cyclone intensity and intensification in a global climate model. *J. Climate*, **31**, 8281–8303, https://doi.org/10.1175/JCLI-D-17-0898.1.

Bian, G.-F., G.-Z. Nie, and X. Qiu, 2021: How well is outer tropical cyclone size represented in the ERA5 reanalysis dataset? *Atmos. Res.*, **249**, 105339, https://doi.org/10.1016/j.atmosres.2020.105339.

Brammer, A., 2017: Tropical cyclone vortex tracker. Zenodo, https://doi.org/10.5281/zenodo.266194.

Bretherton, C. S., M. Widmann, V. P. Dymnikov, J. M. Wallace, and I. Bladé, 1999: The effective number of spatial degrees of freedom of a time-varying field. *J. Climate*, **12**, 1990–2009, https://doi.org/10.1175/1520-0442(1999)012<1990:TENOSD>2.0.CO;2.

Carrasco, C. A., C. W. Landsea, and Y.-L. Lin, 2014: The influence of tropical cyclone size on its intensification. *Wea. Forecasting*, **29**, 582–590, https://doi.org/10.1175/WAF-D-13-00092.1.

Chavas, D. R., and K. A. Emanuel, 2010: A QuikSCAT climatology of tropical cyclone size. *Geophys. Res. Lett.*, **37**, L18816, https://doi.org/10.1029/2010GL044558.

——, and ——, 2014: Equilibrium tropical cyclone size in an idealized state of axisymmetric radiative–convective equilibrium. *J. Atmos. Sci.*, **71**, 1663–1680, https://doi.org/10.1175/JAS-D-13-0155.1.

——, and J. Vigh, 2014: QSCAT-R: The QuikSCAT tropical cyclone radial structure dataset. NCAR Tech. Note NCAR/TN-513+STR, 25 pp., https://verif.rap.ucar.edu/tcdata/quikscat/dataset/index.php.

——, and N. Lin, 2016: A model for the complete radial structure of the tropical cyclone wind field. Part II: Wind field variability. *J. Atmos. Sci.*, **73**, 3093–3113, https://doi.org/10.1175/JAS-D-15-0185.1.

——, and K. A. Reed, 2019: Dynamical aquaplanet experiments with uniform thermal forcing: System dynamics and implications for tropical cyclone genesis and size. *J. Atmos. Sci.*, **76**, 2257–2274, https://doi.org/10.1175/JAS-D-19-0001.1.

——, and J. A. Knaff, 2022: A simple model for predicting the tropical cyclone radius of maximum wind from outer size. *Wea. Forecasting*, **37**, 563–579, https://doi.org/10.1175/WAF-D-21-0103.1.

——, N. Lin, and K. Emanuel, 2015: A model for the complete radial structure of the tropical cyclone wind field. Part I: Comparison with observed structure. *J. Atmos. Sci.*, **72**, 3647–3662, https://doi.org/10.1175/JAS-D-15-0014.1.

——, ——, W. Dong, and Y. Lin, 2016: Observed tropical cyclone size revisited. *J. Climate*, **29**, 2923–2939, https://doi.org/10.1175/JCLI-D-15-0731.1.

——, K. A. Reed, and J. A. Knaff, 2017: Physical understanding of the tropical cyclone wind–pressure relationship. *Nat. Commun.*, **8**, 1360, https://doi.org/10.1038/s41467-017-01546-9.

Chen, D. Y.-C., K. K. W. Cheung, and C.-S. Lee, 2011: Some implications of core regime wind structures in western North Pacific tropical cyclones. *Wea. Forecasting*, **26**, 61–75, https://doi.org/10.1175/2010WAF2222420.1.

Chen, J., and D. R. Chavas, 2020: The transient responses of an axisymmetric tropical cyclone to instantaneous surface roughening and drying. *J. Atmos. Sci.*, **77**, 2807–2834, https://doi.org/10.1175/JAS-D-19-0320.1.

Cocks, S. B., and W. M. Gray, 2002: Variability of the outer wind profiles of western North Pacific typhoons: Classifications and techniques for analysis and forecasting. *Mon. Wea. Rev.*, **130**, 1989–2005, https://doi.org/10.1175/1520-0493(2002)130<1989:VOTOWP>2.0.CO;2.

Davis, C. A., 2018: Resolving tropical cyclone intensity in models. *Geophys. Res. Lett.*, **45**, 2082–2087, https://doi.org/10.1002/2017GL076966.

DeMaria, M., 1996: The effect of vertical shear on tropical cyclone intensity change. *J. Atmos. Sci.*, **53**, 2076–2088, https://doi.org/10.1175/1520-0469(1996)053<2076:TEOVSO>2.0.CO;2.

Diamantakis, M., and L. Magnusson, 2016: Sensitivity of the ECMWF model to semi-Lagrangian departure point iterations. *Mon. Wea. Rev.*, **144**, 3233–3250, https://doi.org/10.1175/MWR-D-15-0432.1.

Emanuel, K., C. DesAutels, C. Holloway, and R. Korty, 2004: Environmental control of tropical cyclone intensity. *J. Atmos. Sci.*, **61**, 843–858, https://doi.org/10.1175/1520-0469(2004)061<0843:ECOTCI>2.0.CO;2.

Evans, C., and Coauthors, 2017: The extratropical transition of tropical cyclones. Part I: Cyclone evolution and direct impacts. *Mon. Wea. Rev.*, **145**, 4317–4344, https://doi.org/10.1175/MWR-D-17-0027.1.

Evans, J. L., and R. E. Hart, 2003: Objective indicators of the life cycle evolution of extratropical transition for Atlantic tropical cyclones. *Mon. Wea. Rev.*, **131**, 909–925, https://doi.org/10.1175/1520-0493(2003)131<0909:OIOTLC>2.0.CO;2.

Ferrier, B. S., 2005: An efficient mixed-phase cloud and precipitation scheme for use in operational NWP models. *Proc. 2005 AGU Spring Meeting*, Abstract 42A–02.

Forbes, R. M., A. M. Tompkins, and A. Untch, 2011: A new prognostic bulk microphysics scheme for the IFS. ECMWF Tech Memo. 649, 28 pp., https://www.ecmwf.int/node/9441.

Franklin, J. L., M. L. Black, and K. Valde, 2003: GPS dropwindsonde wind profiles in hurricanes and their operational implications. *Wea. Forecasting*, **18**, 32–44, https://doi.org/10.1175/1520-0434(2003)018<0032:GDWPIH>2.0.CO;2.

Freidenreich, S. M., and V. Ramaswamy, 1999: A new multiple-band solar radiative parameterization for general circulation models. *J. Geophys. Res.*, **104**, 31 389–31 409, https://doi.org/10.1029/1999JD900456.

Gopalakrishnan, S. G., F. Marks Jr., X. Zhang, J.-W. Bao, K.-S. Yeh, and R. Atlas, 2011: The experimental HWRF system: A study on the influence of horizontal resolution on the structure and intensity changes in tropical cyclones using an idealized framework. *Mon. Wea. Rev.*, **139**, 1762–1784, https://doi.org/10.1175/2010MWR3535.1.

——, ——, J. A. Zhang, X. Zhang, J.-W. Bao, and V. Tallapragada, 2013: A study of the impacts of vertical diffusion on the structure and intensity of the tropical cyclones using the high-resolution HWRF system. *J. Atmos. Sci.*, **70**, 524–541, https://doi.org/10.1175/JAS-D-11-0340.1.

Gori, A., N. Lin, D. Xi, and K. Emanuel, 2022: Tropical cyclone climatology change greatly exacerbates US extreme rainfall–surge hazard. *Nat. Climate Change*, **12**, 171–178, https://doi.org/10.1038/s41558-021-01272-7.

Haarsma, R. J., and Coauthors, 2016: High Resolution Model Intercomparison Project (HighResMIP v1. 0) for CMIP6. *Geosci. Model Dev.*, **9**, 4185–4208, https://doi.org/10.5194/gmd-9-4185-2016.

Harris, L. M., S.-J. Lin, and C. Tu, 2016: High-resolution climate simulations using GFDL HiRAM with a stretched global grid. *J. Climate*, **29**, 4293–4314, https://doi.org/10.1175/JCLI-D-15-0389.1.

Hart, R. E., 2003: A cyclone phase space derived from thermal wind and thermal asymmetry. *Mon. Wea. Rev.*, **131**, 585–616, https://doi.org/10.1175/1520-0493(2003)131<0585:ACPSDF>2.0.CO;2.

——, and J. L. Evans, 2001: A climatology of the extratropical transition of Atlantic tropical cyclones. *J. Climate*, **14**, 546–564, https://doi.org/10.1175/1520-0442(2001)014<0546:ACOTET>2.0.CO;2.

——, ——, and C. Evans, 2006: Synoptic composites of the extratropical transition life cycle of North Atlantic tropical cyclones: Factors determining posttransition evolution. *Mon. Wea. Rev.*, **134**, 553–578, https://doi.org/10.1175/MWR3082.1.

Hazelton, A., and Coauthors, 2021: 2019 Atlantic hurricane forecasts from the global-nested hurricane analysis and forecast system: Composite statistics and key events. *Wea. Forecasting*, **36**, 519–538, https://doi.org/10.1175/WAF-D-20-0044.1.

——, and Coauthors, 2022: Performance of 2020 real-time Atlantic hurricane forecasts from high-resolution global-nested hurricane models: HAFS-globalnest and GFDL T-SHiELD. *Wea. Forecasting*, **37**, 143–161, https://doi.org/10.1175/WAF-D-21-0102.1.

Held, I. M., and V. D. Larichev, 1996: A scaling theory for horizontally homogeneous, baroclinically unstable flow on a beta plane. *J. Atmos. Sci.*, **53**, 946–952, https://doi.org/10.1175/1520-0469(1996)053<0946:ASTFHH>2.0.CO;2.

Hersbach, H., and Coauthors, 2020: The ERA5 global reanalysis. *Quart. J. Roy. Meteor. Soc.*, **146**, 1999–2049, https://doi.org/10.1002/qj.3803.

Hill, K. A., and G. M. Lackmann, 2009: Influence of environmental humidity on tropical cyclone size. *Mon. Wea. Rev.*, **137**, 3294–3315, https://doi.org/10.1175/2009MWR2679.1.

Hlywiak, J., and D. S. Nolan, 2021: The response of the near-surface tropical cyclone wind field to inland surface roughness length and soil moisture content during and after landfall. *J. Atmos. Sci.*, **78**, 983–1000, https://doi.org/10.1175/JAS-D-20-0211.1.

Hsieh, T.-L., G. A. Vecchi, W. Yang, I. M. Held, and S. T. Garner, 2020: Large-scale control on the frequency of tropical cyclones and seeds: A consistent relationship across a hierarchy of global atmospheric models. *Climate Dyn.*, **55**, 3177–3196, https://doi.org/10.1007/s00382-020-05446-5.

Irish, J. L., D. T. Resio, and J. J. Ratcliff, 2008: The influence of storm size on hurricane surge. *J. Phys. Oceanogr.*, **38**, 2003–2013, https://doi.org/10.1175/2008JPO3727.1.

Jones, S. C., 1995: The evolution of vortices in vertical shear. Part I: Initially barotropic vortices. *Quart. J. Roy. Meteor. Soc.*, **121**, 821–851, https://doi.org/10.1002/qj.49712152406.

——, and Coauthors, 2003: The extratropical transition of tropical cyclones: Forecast challenges, current understanding, and future directions. *Wea. Forecasting*, **18**, 1052–1092, https://doi.org/10.1175/1520-0434(2003)018<1052:TETOTC>2.0.CO;2.

Kalnay, E., and Coauthors, 1996: The NCEP/NCAR 40-Year Reanalysis Project. *Bull. Amer. Meteor. Soc.*, **77**, 437–472, https://doi.org/10.1175/1520-0477(1996)077<0437:TNYRP>2.0.CO;2.

Kim, H.-S., G. A. Vecchi, T. R. Knutson, W. G. Anderson, T. L. Delworth, A. Rosati, F. Zeng, and M. Zhao, 2014: Tropical

cyclone simulation and response to CO_2 doubling in the GFDL CM2.5 high-resolution coupled climate model. *J. Climate*, **27**, 8034–8054, https://doi.org/10.1175/JCLI-D-13-00475.1.

Knaff, J. A., S. P. Longmore, and D. A. Molenar, 2014: An objective satellite-based tropical cyclone size climatology. *J. Climate*, **27**, 455–476, https://doi.org/10.1175/JCLI-D-13-00096.1.

——, C. R. Sampson, and G. Chirokova, 2017: A global statistical–dynamical tropical cyclone wind radii forecast scheme. *Wea. Forecasting*, **32**, 629–644, https://doi.org/10.1175/WAF-D-16-0168.1.

——, ——, and K. D. Musgrave, 2018: An operational rapid intensification prediction aid for the western North Pacific. *Wea. Forecasting*, **33**, 799–811, https://doi.org/10.1175/WAF-D-18-0012.1.

——, ——, and B. R. Strahl, 2020: A tropical cyclone rapid intensification prediction aid for the Joint Typhoon Warning Center's areas of responsibility. *Wea. Forecasting*, **35**, 1173–1185, https://doi.org/10.1175/WAF-D-19-0228.1.

Knapp, K. R., M. C. Kruk, D. H. Levinson, H. J. Diamond, and C. J. Neumann, 2010: The International Best Track Archive for Climate Stewardship (IBTrACS). *Bull. Amer. Meteor. Soc.*, **91**, 363–376, https://doi.org/10.1175/2009BAMS2755.1.

Knutson, T. R., J. J. Sirutis, S. T. Garner, I. M. Held, and R. E. Tuleya, 2007: Simulation of the recent multidecadal increase of Atlantic hurricane activity using an 18-km-grid regional model. *Bull. Amer. Meteor. Soc.*, **88**, 1549–1565, https://doi.org/10.1175/BAMS-88-10-1549.

——, and Coauthors, 2010: Tropical cyclones and climate change. *Nat. Geosci.*, **3**, 157–163, https://doi.org/10.1038/ngeo779.

——, and Coauthors, 2013: Dynamical downscaling projections of twenty-first-century Atlantic hurricane activity: CMIP3 and CMIP5 model-based scenarios. *J. Climate*, **26**, 6591–6617, https://doi.org/10.1175/JCLI-D-12-00539.1.

——, J. J. Sirutis, M. Zhao, R. E. Tuleya, M. Bender, G. A. Vecchi, G. Villarini, and D. Chavas, 2015: Global projections of intense tropical cyclone activity for the late twenty-first century from dynamical downscaling of CMIP5/RCP4.5 scenarios. *J. Climate*, **28**, 7203–7224, https://doi.org/10.1175/JCLI-D-15-0129.1.

——, and Coauthors, 2020: Tropical cyclones and climate change assessment: Part II: Projected response to anthropogenic warming. *Bull. Amer. Meteor. Soc.*, **101**, E303–E322, https://doi.org/10.1175/BAMS-D-18-0194.1.

——, J. J. Sirutis, M. A. Bender, R. E. Tuleya, and B. A. Schenkel, 2022: Dynamical downscaling projections of late twenty-first-century U.S. landfalling hurricane activity. *Climatic Change*, **171**, 28, https://doi.org/10.1007/s10584-022-03346-7.

Kofron, D. E., E. A. Ritchie, and J. S. Tyo, 2010: Determination of a consistent time for the extratropical transition of tropical cyclones. Part II: Potential vorticity metrics. *Mon. Wea. Rev.*, **138**, 4344–4361, https://doi.org/10.1175/2010MWR3181.1.

Kreussler, P., and Coauthors, 2021: Tropical cyclone integrated kinetic energy in an ensemble of HighResMIP simulations. *Geophys. Res. Lett.*, **48**, e2020GL090963, https://doi.org/10.1029/2020GL090963.

Kurihara, Y., R. E. Tuleya, and M. A. Bender, 1998: The GFDL hurricane prediction system and its performance in the 1995 hurricane season. *Mon. Wea. Rev.*, **126**, 1306–1322, https://doi.org/10.1175/1520-0493(1998)126<1306:TGHPSA>2.0.CO;2.

Lacis, A. A., and J. Hansen, 1974: A parameterization for the absorption of solar radiation in the earth's atmosphere. *J. Atmos. Sci.*, **31**, 118–133, https://doi.org/10.1175/1520-0469(1974)031<0118:APFTAO>2.0.CO;2.

Lee, C.-S., K. K. W. Cheung, W.-T. Fang, and R. L. Elsberry, 2010: Initial maintenance of tropical cyclone size in the western North Pacific. *Mon. Wea. Rev.*, **138**, 3207–3223, https://doi.org/10.1175/2010MWR3023.1.

Lin, N., and D. Chavas, 2012: On hurricane parametric wind and applications in storm surge modeling. *J. Geophys. Res.*, **117**, D09120, https://doi.org/10.1029/2011JD017126.

——, P. Lane, K. A. Emanuel, R. M. Sullivan, and J. P. Donnelly, 2014: Heightened hurricane surge risk in northwest Florida revealed from climatological-hydrodynamic modeling and paleorecord reconstruction. *J. Geophys. Res. Atmos.*, **119**, 8606–8623, https://doi.org/10.1002/2014JD021584.

Lin, S.-J., 2004: A "vertically Lagrangian" finite-volume dynamical core for global models. *Mon. Wea. Rev.*, **132**, 2293–2307, https://doi.org/10.1175/1520-0493(2004)132<2293:AVLFDC>2.0.CO;2.

Lin, Y., M. Zhao, and M. Zhang, 2015: Tropical cyclone rainfall area controlled by relative sea surface temperature. *Nat. Commun.*, **6**, 6591, https://doi.org/10.1038/ncomms7591.

Liu, M., G. A. Vecchi, J. A. Smith, and H. Murakami, 2017: The present-day simulation and twenty-first-century projection of the climatology of extratropical transition in the North Atlantic. *J. Climate*, **30**, 2739–2756, https://doi.org/10.1175/JCLI-D-16-0352.1.

Lu, K. Y., and D. R. Chavas, 2022: Tropical cyclone size is strongly limited by the Rhines scale: Experiments with a barotropic model. *J. Atmos. Sci.*, **79**, 2109–2124, https://doi.org/10.1175/JAS-D-21-0224.1.

Lu, P., N. Lin, K. Emanuel, D. Chavas, and J. Smith, 2018: Assessing hurricane rainfall mechanisms using a physics-based model: Hurricanes Isabel (2003) and Irene (2011). *J. Atmos. Sci.*, **75**, 2337–2358, https://doi.org/10.1175/JAS-D-17-0264.1.

Marchok, T. P., 2002: How the NCEP tropical cyclone tracker works. *Proc. 25th Conf. on Hurricanes and Tropical Meteorology*, San Diego, CA, Amer. Meteor. Soc., P1.13, https://ams.confex.com/ams/25HURR/techprogram/paper_37628.htm.

Marsooli, R., N. Lin, K. Emanuel, and K. Feng, 2019: Climate change exacerbates hurricane flood hazards along US Atlantic and Gulf coasts in spatially varying patterns. *Nat. Commun.*, **10**, 3785, https://doi.org/10.1038/s41467-019-11755-z.

Martinez, J., C. C. Nam, and M. M. Bell, 2020: On the contributions of incipient vortex circulation and environmental moisture to tropical cyclone expansion. *J. Geophys. Res. Atmos.*, **125**, e2020JD033324, https://doi.org/10.1029/2020JD033324.

McCaul, E. W., Jr., 1991: Buoyancy and shear characteristics of hurricane-tornado environments. *Mon. Wea. Rev.*, **119**, 1954–1978, https://doi.org/10.1175/1520-0493(1991)119<1954:BASCOH>2.0.CO;2.

Meehl, G. A., C. Covey, T. Delworth, M. Latif, B. McAvaney, J. F. B. Mitchell, R. J. Stouffer, and K. E. Taylor, 2007: The WCRP CMIP3 multimodel dataset: A new era in climate change research. *Bull. Amer. Meteor. Soc.*, **88**, 1383–1394, https://doi.org/10.1175/BAMS-88-9-1383.

Merrill, R. T., 1984: A comparison of large and small tropical cyclones. *Mon. Wea. Rev.*, **112**, 1408–1418, https://doi.org/10.1175/1520-0493(1984)112<1408:ACOLAS>2.0.CO;2.

Michaelis, A. C., and G. M. Lackmann, 2019: Climatological changes in the extratropical transition of tropical cyclones in high-resolution global simulations. *J. Climate*, **32**, 8733–8753, https://doi.org/10.1175/JCLI-D-19-0259.1.

Mok, D. K. H., J. C. L. Chan, and K. T. F. Chan, 2018: A 31-year climatology of tropical cyclone size from the NCEP Climate Forecast System Reanalysis. *Int. J. Climatol.*, **38**, e796–e806, https://doi.org/10.1002/joc.5407.

Moorthi, S., and M. J. Suarez, 1992: Relaxed Arakawa-Schubert. A parameterization of moist convection for general circulation models. *Mon. Wea. Rev.*, **120**, 978–1002, https://doi.org/10.1175/1520-0493(1992)120<0978:RASAPO>2.0.CO;2.

Morcrette, J. J., H. W. Barker, J. N. S. Cole, M. J. Iacono, and R. Pincus, 2008: Impact of a new radiation package, McRad, in the ECMWF Integrated Forecasting System. *Mon. Wea. Rev.*, **136**, 4773–4798, https://doi.org/10.1175/2008MWR2363.1.

Murakami, H., and Coauthors, 2015: Simulation and prediction of category 4 and 5 hurricanes in the high-resolution GFDL HiFLOR coupled climate model. *J. Climate*, **28**, 9058–9079, https://doi.org/10.1175/JCLI-D-15-0216.1.

——, and Coauthors, 2016: Seasonal forecasts of major hurricanes and landfalling tropical cyclones using a high-resolution GFDL coupled climate model. *J. Climate*, **29**, 7977–7989, https://doi.org/10.1175/JCLI-D-16-0233.1.

Neelin, J. D., M. Münnich, H. Su, J. E. Meyerson, and C. E. Holloway, 2006: Tropical drying trends in global warming models and observations. *Proc. Natl. Acad. Sci. USA*, **103**, 6110–6115, https://doi.org/10.1073/pnas.0601798103.

Pan, H.-L., and W.-S. Wu, 1995: Implementing a mass flux convection parameterization package for the NMC medium-range forecast model. NMC Office Note 409, NOAA, 43 pp., https://repository.library.noaa.gov/view/noaa/11429.

Paredes, M., B. A. Schenkel, R. Edwards, and M. Coniglio, 2021: Tropical cyclone outer size impacts the number and location of tornadoes. *Geophys. Res. Lett.*, **48**, e2021GL095922, https://doi.org/10.1029/2021GL095922.

Pendergrass, A. G., R. Knutti, F. Lehner, C. Deser, and B. M. Sanderson, 2017: Precipitation variability increases in a warmer climate. *Sci. Rep.*, **7**, 17966, https://doi.org/10.1038/s41598-017-17966-y.

Powell, M. D., and T. A. Reinhold, 2007: Tropical cyclone destructive potential by integrated kinetic energy. *Bull. Amer. Meteor. Soc.*, **88**, 513–526, https://doi.org/10.1175/BAMS-88-4-513.

——, P. J. Vickery, and T. A. Reinhold, 2003: Reduced drag coefficient for high wind speeds in tropical cyclones. *Nature*, **422**, 279–283, https://doi.org/10.1038/nature01481.

Rayner, N. A., D. E. Parker, E. B. Horton, C. K. Folland, L. V. Alexander, D. P. Rowell, E. C. Kent, and A. Kaplan, 2003: Global analyses of sea surface temperature, sea ice, and night marine air temperature since the late nineteenth century. *J. Geophys. Res.*, **108**, 4407, https://doi.org/10.1029/2002JD002670.

Rhines, P. B., 1975: Waves and turbulence on a beta-plane. *J. Fluid Mech.*, **69**, 417–443, https://doi.org/10.1017/S0022112075001504.

Rotstayn, L. D., 1997: A physically based scheme for the treatment of stratiform clouds and precipitation in large-scale models. I: Description and evaluation of the microphysical processes. *Quart. J. Roy. Meteor. Soc.*, **123**, 1227–1282, https://doi.org/10.1002/qj.49712354106.

Rotunno, R., and K. A. Emanuel, 1987: An air–sea interaction theory for tropical cyclones. Part II: Evolutionary study using a nonhydrostatic axisymmetric numerical model. *J. Atmos. Sci.*, **44**, 542–561, https://doi.org/10.1175/1520-0469(1987)044<0542:AAITFT>2.0.CO;2.

Schenkel, B. A., and R. E. Hart, 2012: An examination of tropical cyclone position, intensity, and intensity life cycle within atmospheric reanalysis datasets. *J. Climate*, **25**, 3453–3475, https://doi.org/10.1175/2011JCLI4208.1.

——, N. Lin, D. Chavas, M. Oppenheimer, and A. Brammer, 2017: Evaluating outer tropical cyclone size in reanalysis datasets using QuikSCAT data. *J. Climate*, **30**, 8745–8762, https://doi.org/10.1175/JCLI-D-17-0122.1.

——, ——, ——, G. A. Vecchi, M. Oppenheimer, and A. Brammer, 2018: Lifetime evolution of outer tropical cyclone size and structure as diagnosed from reanalysis and climate model data. *J. Climate*, **31**, 7985–8004, https://doi.org/10.1175/JCLI-D-17-0630.1.

Schwarzkopf, M. D., and S. B. Fels, 1991: The simplified exchange method revisited: An accurate, rapid method for computation of infrared cooling rates and fluxes. *J. Geophys. Res.*, **96**, 9075–9096, https://doi.org/10.1029/89JD01598.

——, and V. Ramaswamy, 1999: Radiative effects of CH_4, N_2O, halocarbons and the foreign-broadened H_2O continuum: A GCM experiment. *J. Geophys. Res.*, **104**, 9467–9488, https://doi.org/10.1029/1999JD900003.

Stansfield, A. M., and K. A. Reed, 2021: Tropical cyclone precipitation response to surface warming in aquaplanet simulations with uniform thermal forcing. *J. Geophys. Res. Atmos.*, **126**, e2021JD035197, https://doi.org/10.1029/2021JD035197.

——, ——, and C. M. Zarzycki, 2020: Changes in precipitation from North Atlantic tropical cyclones under RCP scenarios in the variable-resolution community atmosphere model. *Geophys. Res. Lett.*, **47**, e2019GL086930, https://doi.org/10.1029/2019GL086930.

Taylor, K. E., R. J. Stouffer, and G. A. Meehl, 2012: An overview of CMIP5 and the experiment design. *Bull. Amer. Meteor. Soc.*, **93**, 485–498, https://doi.org/10.1175/BAMS-D-11-00094.1.

Tiedtke, M., 1989: A comprehensive mass flux scheme for cumulus parameterization in large-scale models. *Mon. Wea. Rev.*, **117**, 1779–1800, https://doi.org/10.1175/1520-0493(1989)117<1779:ACMFSF>2.0.CO;2.

Ting, M., J. P. Kossin, S. J. Camargo, and C. Li, 2019: Past and future hurricane intensity change along the U.S. east coast. *Sci. Rep.*, **9**, 7795, https://doi.org/10.1038/s41598-019-44252-w.

Tomita, H., and M. Satoh, 2004: A new dynamical framework of nonhydrostatic global model using the icosahedral grid. *Fluid Dyn. Res.*, **34**, 357–400, https://doi.org/10.1016/j.fluiddyn.2004.03.003.

Torn, R. D., and C. Snyder, 2012: Uncertainty of tropical cyclone best-track information. *Wea. Forecasting*, **27**, 715–729, https://doi.org/10.1175/WAF-D-11-00085.1.

Ventura, V., C. J. Paciorek, and J. S. Risbey, 2004: Controlling the proportion of falsely rejected hypotheses when conducting multiple tests with climatological data. *J. Climate*, **17**, 4343–4356, https://doi.org/10.1175/3199.1.

Walsh, K. J. E., M. Fiorino, C. W. Landsea, and K. L. McInnes, 2007: Objectively determined resolution-dependent threshold criteria for the detection of tropical cyclones in climate models and reanalyses. *J. Climate*, **20**, 2307–2314, https://doi.org/10.1175/JCLI4074.1.

Wang, D., Y. Lin, and D. R. Chavas, 2022: Tropical cyclone potential size. *J. Atmos. Sci.*, https://doi.org/10.1175/JAS-D-21-0325.1, in press.

Weatherford, C. L., and W. M. Gray, 1988: Typhoon structure as revealed by aircraft reconnaissance. Part I: Data analysis and climatology. *Mon. Wea. Rev.*, **116**, 1032–1043, https://doi.org/10.1175/1520-0493(1988)116<1032:TSARBA>2.0.CO;2.

Wilks, D. S., 2016: "The stippling shows statistically significant grid points": How research results are routinely overstated and overinterpreted, and what to do about it. *Bull. Amer. Meteor. Soc.*, **97**, 2263–2273, https://doi.org/10.1175/BAMS-D-15-00267.1.

Xu, J., and Y. Wang, 2010: Sensitivity of the simulated tropical cyclone inner-core size to the initial vortex size. *Mon. Wea. Rev.*, **138**, 4135–4157, https://doi.org/10.1175/2010MWR3335.1.

Yamada, Y., M. Satoh, M. Sugi, C. Kodama, A. T. Noda, M. Nakano, and T. Nasuno, 2017: Response of tropical cyclone activity and structure to global warming in a high-resolution global nonhydrostatic model. *J. Climate*, **30**, 9703–9724, https://doi.org/10.1175/JCLI-D-17-0068.1.

Yang, W., T.-L. Hsieh, and G. A. Vecchi, 2021: Hurricane annual cycle controlled by both seeds and genesis probability. *Proc. Natl. Acad. Sci. USA*, **118**, e2108397118, https://doi.org/10.1073/pnas.2108397118.

Zhang, K., and K. T. Chan, 2022: An ERA5 global climatology of tropical cyclone size asymmetry. *Int. J. Climatol.*, https://doi.org/10.1002/joc.7846, in press.

Zhao, M., I. M. Held, S.-J. Lin, and G. A. Vecchi, 2009: Simulations of global hurricane climatology, interannual variability, and response to global warming using a 50-km resolution GCM. *J. Climate*, **22**, 6653–6678, https://doi.org/10.1175/2009JCLI3049.1.